

# A new zoroasterid asteroid from the Eocene of Seymour Island, Antarctica

EVANGELINA E. PALÓPOLO, SOLEDAD S. BREZINA, SILVIO CASADIO, MIGUEL GRIFFIN,  
and SERGIO SANTILLANA



Palópolo, E.E., Brezina, S.S., Casadio, S., Griffin, M., and Santillana, S. 2021. A new zoroasterid asteroid from the Eocene of Seymour Island, Antarctica. *Acta Palaeontologica Polonica* 66 (X): xxx–xxx.

New, well-preserved fossil starfish material is recorded from the Eocene La Meseta Formation exposed in Seymour Island, Antarctica. The use of new technology (i.e., microCT) on several fragments enabled the visualization of new characters and the differentiation of a new species, *Zoroaster marambioensis* sp. nov., which was previously identified as *Zoroaster* aff. *Z. fulgens*. Diagnostic characters of *Z. marambioensis* sp. nov. are (i) central disc plate enlarged, lobate and flattened, (ii) disc ring with enlarged, tumid radials and polygonal, flattened inter-radials, (iii) primary spines on disc only present on radials, (iv) oral armature with 1–3 primary spines and 1–2 secondary spines for each prominent adambulacral. The depositional setting represents the outer zone of an estuary dominated by marine processes affected by long lived hyperpycnal flows. We argue that zoroasterids colonized a distal part of the estuary under normal marine salinity and were killed by the input of freshwater carried by a hyperpycnal flow, and immediately buried by fine grained sandstone. Sedimentological data suggest that *Z. marambioensis* sp. nov. lived in shallow-water environments, it seems possible that they were adapted to higher temperatures than other Recent species of the genus, which inhabit cold, deep marine environments.

**Key words:** Asteroidea, Zoroasteridae, palaeoenvironment, Paleogene, La Meseta Formation, Antarctic Peninsula.

*Evangelina E. Palópolo* [eepalopolo@unrn.edu.ar] and *Silvio Casadio* [scasadio@unrn.edu.ar], *Universidad Nacional de Río Negro, Instituto de Investigación en Paleobiología y Geología, Río Negro, Argentina; and IIPG. UNRN. Consejo Nacional de Investigaciones científicas y Tecnológicas (CONICET), Av. Roca 1242, (R8332EXZ) General Roca, Río Negro, Argentina.*

*Soledad S. Brezina* [sbrezina@unrn.edu.ar], *Universidad Nacional de Río Negro, Instituto de Investigación en Paleobiología y Geología, Río Negro, Argentina.*

*Miguel Griffin* [mgriffin@fcnym.unlp.edu.ar], *Facultad de Ciencias Naturales y Museo, Universidad Nacional de La Plata, Edificio Anexo Laboratorios Museo (Laboratorio 110), Avenida 122 y 60, La Plata, Buenos Aires, Argentina.*

*Sergio Santillana* [ssantillana@dna.gov.ar], *Instituto Antártico Argentino, 25 de Mayo 1143, San Martín, provincia de Buenos Aires, Argentina.*

Received 6 December 2019, accepted 12 December 2020, available online 7 June 2021.

Copyright © 2021 E.E. Palópolo et al. This is an open-access article distributed under the terms of the Creative Commons Attribution License (for details please see <http://creativecommons.org/licenses/by/4.0/>), which permits unrestricted use, distribution, and reproduction in any medium, provided the original author and source are credited.

## Introduction

Zoroasterids (the family Zoroasteridae Sladen, 1889) comprise a group of starfishes with five rays, a small disc, long and tapering arms, and skeletal plates arranged in series (both transverse and longitudinal) covered by primary and secondary spines (McKnight 2006). Species of this family also have a single marginal row, papular pores arranged on longitudinal and transverse series, imbricated or reticulated disc and arm plate arrangement, actinolateral spines larger than other primary spines, adpressed or facing abactinally, straight pedicellariae (except in *Pholidaster*), adambulacrals

alternately carinate, and tube feet in four rows becoming two rows distally (Blake 1987; Mah 2000, 2007; Mah and Foltz 2011; Mah and Blake 2012; Fau and Villier 2018).

The family was originally defined by Sladen (1889), and includes eight genera (one of them with only fossil representatives) and 35 nominal species inhabiting abyssal and bathyal environments of the Atlantic, Pacific and Indian oceans (Mah 2007).

The fossil record of the family Zoroasteridae is scarce. Relatively few species are known, including one from the Jurassic of Europe (Hess 1974; Villier et al. 2009), two from the Eocene of Antarctica and New Zealand (Blake and Zinsmeister 1979, 1988; Blake and Aronson 1998; Eagle

2006; this article), and one from the Miocene of Japan (Kato and Oji 2013). These records are highly biased because of their body plan (i.e., the small disc, the very long arms and weak ossicle connection).

Echinoderm ossicles are connected by muscles, ligaments, interlocking stereom, cement or a combination of these (Ausich et al. 2001). Because starfishes have a large coelomic cavity that extends into each arm (Ferguson 1992; Brusca and Brusca 2003) and most show a weakly articulated body skeleton, they are prone to complete disarticulation within few days after death (Brett et al. 1997) due to soft tissue decomposition and skeletal collapse. The fact that ossicle fusion in asteroids is far from that achieved in echinoids is a key feature contributing to disarticulation. Yet, in zoroasterids ossicles are quite firmly tied together relative to other asteroids, a fact that could somewhat enhance their preservation potential. However, we consider that a simple stratum containing several specimens of almost complete asteroids in living position would still be considered an exceptionally preserved deposit (Brett et al. 1997), even in the case of zoroasterids in which ossicles are more closely tied together than in other asteroids. This type of preservation provides important information about paleobiology, paleoecology, sedimentary environment and taphonomic history of the remains (Brett 1978).

The systematics of the group has been studied deeply based on Recent species but many questions remain regarding its origin and evolution because of its poor fossil record. Previous authors discussed the possible origin of the family in the Wedellian Province and its subsequent biogeographical history (Blake 1987, 1990; Mah 2007; Villier et al. 2009; Gale 2011; Mah and Foltz 2011; Mah and Blake 2012). Phylogenetic studies of the Asteroidea place the Zoroasteridae as a basal clade within the or-

der Forcipulatida, based on characters intermediate between the Paleozoic and post-Paleozoic Asteroidea, such as a single marginal series and the arrangement of arm ossicles and spines (Blake 1987, 1990; Mah 2000, 2007; Mah and Foltz 2011; Mah and Blake 2012). Among the Zoroasteridae, the genus *Zoroaster* Wyville Thomson, 1873, shows more derived skeletal characters (e.g., imbricate and well-armored skeleton) than *Myxoderma* Fisher, 1905, and *Sagenaster* Mah, 2007, which have reticulated and open skeletons (Mah 2007).

Primary spines, secondary spines and pedicellariae, together with soft tissues, have been widely used in Recent asteroid systematics. Shape, size and arrangement of these structures are important for identification of zoroasterid species (Downey 1970; Blake 1987; Clark and Downey 1992, among others). Nevertheless, some species of the family have different morphotypes that render taxonomic identification difficult (Howell et al. 2004). Specimens analyzed herein are preserved in detail; both oral and aboral surface characters can be identified, spines and pedicellariae are often in life position. This evidence allowed us to identify dependable characters and to describe a new species of *Zoroaster*, previously reported by Blake and Zinsmeister (1979) as *Zoroaster* aff. *Z. fulgens*, from the La Meseta Formation (Eocene, Antarctic Peninsula).

*Institutional abbreviations.*—IAA, Instituto Antártico Argentina, San Martín, Buenos Aires, Argentina; IAA-Pi, Colección Paleontología de Invertebrados, Repositorio Antártico de Colecciones Paleontológicas y Geológicas del Instituto Antártico Argentino, San Martín, Buenos Aires, Argentina; IIPG, Instituto de Investigación en Paleobiología y Geología, General Roca, Río Negro, Argentina; RAA, Repositorio Antártico de Colecciones Paleontológicas y

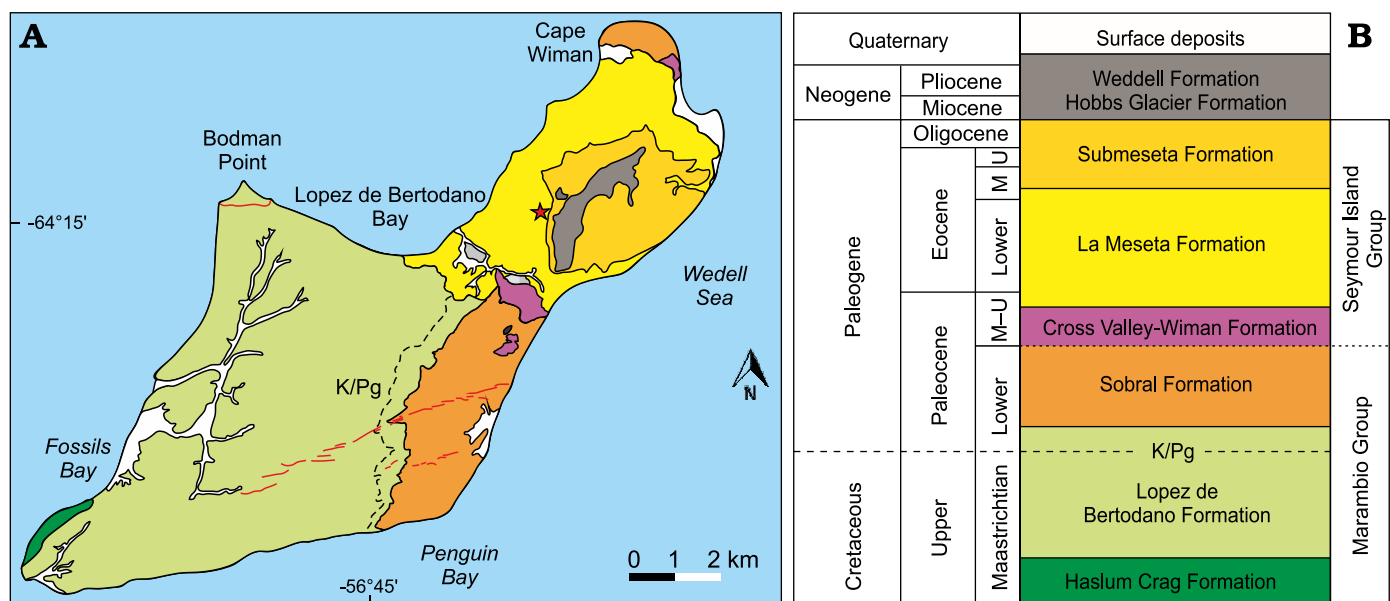


Fig. 1. Geologic map (A) and stratigraphic column (B) of Seymour Island, Antarctica (modified from Montes et al. 2013). The star shows the place of discovery. Abbreviations: M, Middle; U, Upper.

Geológicas del IAA, San Martín, Buenos Aires, Argentina; UNAM, Universidad Nacional Autónoma de México, Ciudad de México, México; UNRN, Universidad Nacional de Río Negro, General Roca, Río Negro, Argentina; YPF, Yacimientos Petrolíferos Fiscales, Buenos Aires, Argentina.

*Nomenclatural acts.*—This published work and the nomenclatural acts it contains, have been registered in ZooBank: urn:lsid:zoobank.org:pub:38AF70B7-F4FE-4166-9DE5-3EC8D68A30E6.

## Geological setting

The La Meseta Formation, exposed in Seymour Island (Fig. 1) off the northern tip of the Antarctic Peninsula, represents the upper part of the infilling of the James Ross Basin and comprises a succession of 250 m of sediments deposited in an incised valley (Montes et al. 2019). Sedimentation took place in estuarine and wave-influenced tidal-shelf environments (Marenssi et al. 1998a; Porębski 2000). The La Meseta Formation is well known for its shell-beds dominated by molluscs but also containing a unique fauna of Antarctic Eocene terrestrial vertebrates that includes several mammals (marsupials, edentates and ungulates) and birds. The fossil associations were the subject of numerous systematic studies (Feldmann and Woodburne 1988; Stilwell and Zinsmeister 1992; Bitner 1996; Goin et al. 1999; Hara 2001). Marenssi et al. (1998a, b) subdivided the La Meseta Formation into six allomembers. From bottom to top these are the Valle de las Focas, Acantilados, Campamento, *Cucullaea* I, *Cucullaea* II and Submeseta allomembers. The depositional setting ranged from a prograding delta front to a storm-influenced subaqueous delta plain dominated by tides after marine-flooding within the incised valley (Marenssi et al. 1998a). The new zoroasterid specimens described in this paper come from the *Cucullaea* I Allomember (Fig. 2). They were collected in an area measuring 20 m<sup>2</sup> (64°14'24" S, 56°40'02" W). The *Cucullaea* I Allomember begins with a shell concentration of several densely- to poorly-packed and poorly-sorted laterally continuous beds, or lenses ranging from 0.5–1.5 m thick, with sharp undulating bases and sharp tops, and trough cross-bedding. Sadler (1988) characterized this shell bed (his Telm 4) by its high content of phosphatic teeth and bones, and suggested it is a transgressive lag distinguished by abundant phosphate pebbles and glauconite. The densely packed beds are dominated by the multiple specimens of bivalve *Cucullaea raea* Zinsmeister, 1984. This concentration represents a tidal channel facies in the outermost part of an estuary (Taylor et al. 2008). In terms of sequence stratigraphy these concentrations represent a tidal ravinement surface. The age of the lower and middle part of the La Meseta Formation is middle Lutetian to Priabonian (Amenábar et al. 2020).

The middle and upper part of the *Cucullaea* I Allomember includes facies of laminated siltstone and fine sandstone

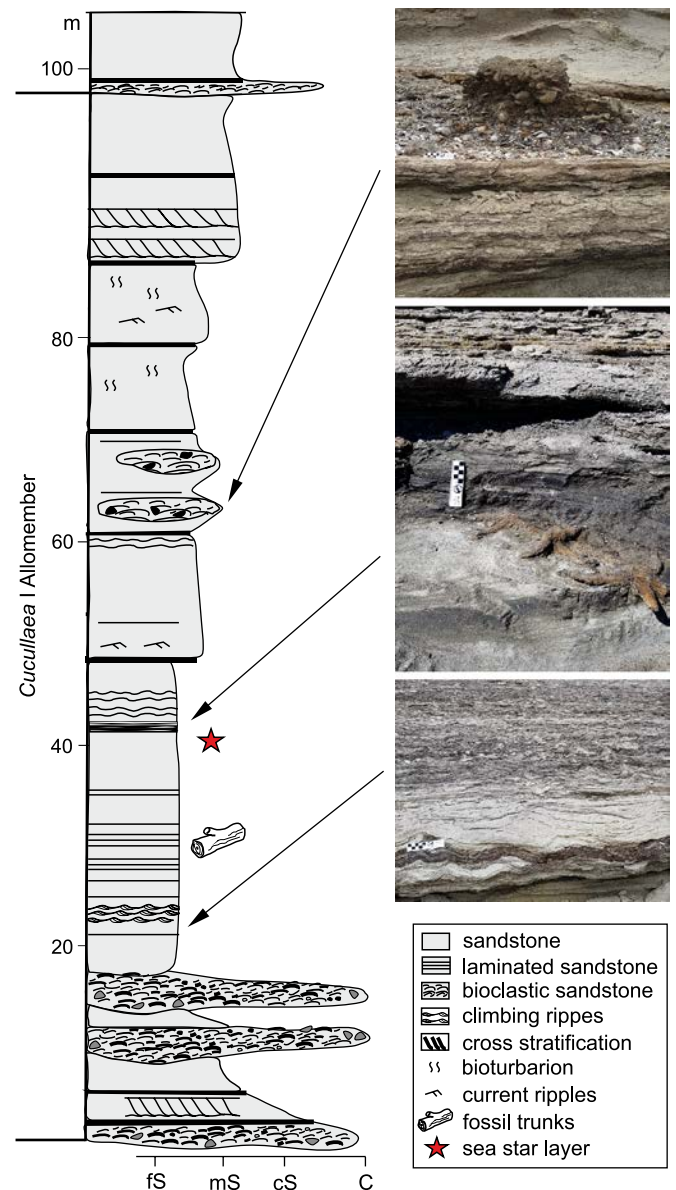


Fig. 2. Detailed stratigraphic column from *Cucullaea* I Allomember, La Meseta Formation. Abbreviations: C, conglomerate; cS, coarse sandstone; fs, fine sandstone; mS, medium sandstone. Scale bars 100 mm.

with climbing ripples, fine grained laminated sandstone and siltstone with trunks, fine grained sandstone with wave ripples and massive fine sandstone. This part of the section represents the outer zone of an estuary dominated by marine processes affected by long lived hyperpycnal flows.

According to Zavala and Pan (2018), the key features of sustained hyperpycnal flows include: (i) an origin associated to a direct fluvial discharge, which is often characterized by long lived flows with fluctuating changes in velocity and concentration, (ii) common occurrence of associated bed-load processes, and (iii) a turbulent flow with a light interstitial fluid (freshwater) together with other light elements in suspension (e.g., charcoal, leaves, and trunks). During a hyperpycnal discharge, freshwater, plant debris and charcoal, are forced to go down and to travel basinwards.



Zoroasterids were collected at the top of a massive fine sandstone bed and they were covered by laminated fine sandstone. Individual laminae are millimeter thick and are intercalated with thin levels with abundant carbonaceous material and even charcoal (Figs. 2, 3). This observation is consistent with the facies L (facies related to flow lofting) hyperpycnal flow facies tract of Zavala et al. (2011).

Lofting rhythmites that cover the zoroasterids are the result of the aggradation of fine-grained materials from suspension clouds related to the buoyant inversion of hyperpycnal flows at flow margin areas (Zavala et al. 2012).

We interpret that the zoroasterids colonized a distal part of the estuary under normal marine salinity and were killed by the input of freshwater carried by a hyperpycnal flow, and immediately buried by fine grained sandstone. The absence of tractive structures in these sandstones suggests an accumulation by normal settling from a suspension cloud elevated over the depositional surface.

## Material and methods

Studied specimens are housed in Colección Paleontología de Invertebrados, Repositorio Antártico de Colecciones Paleontológicas y Geológicas, Instituto Antártico Argentino (IAA) under IAA-Pi-373 code.

While the fossil starfishes were fairly complete in the outcrop, because of their brittleness they suffered some breakage during collection and transport. About 250 fragments were analyzed, most of them preserved in detail. No further treatment was required for fossils except washing and brushing to remove sediment grains attached mostly to the oral surface of skeletons. Pores of the madreporic plate are filled by sediment grains that cannot be removed. Fragments were observed under binocular microscope on both oral and aboral surfaces. Four fragments were observed using Zeiss® Scanning Electronic Microscope (SEM), model Evo MA 15, with variable pressure. MicroCT scans were made with other three fragments using MicroCT Bruker SkyScan 1173 (Pixel size: 50µm, Source Voltage: 110 kV, Source Current: 72 uA) at the Laboratorio de Química Analítica, YPF Tecnología (La Plata, Buenos Aires). Image reconstruction was made using Nrecon 1.6.9.8 software (Filter: Haming, Beam Hardening Correction: 10%, Cone-beam Angle: 17.544950°). A total of 1086, 1098, and 1111 slices were recovered from fragments 1, 2, and 3, respectively. MicroCT image sets were processed using 3D Slicer 4.8.1 (Fedorov et al. 2012) and Drishti 2.6.3 (Limaye 2012) software (SOM 2).

On the basis of original and extended descriptions (Alcock 1893; Ludwig 1905; Fisher 1905, 1906, 1916, 1919, 1928; Clark 1913, 1916, 1920; Clark and Downey 1992; Esteban-Vasquez 2018), nine new characters were added to the zoroasterid phylogenetic matrix published by Mah (2007). These were considered by the authors as dependable characters for the species of *Zoroaster*. Characters of *Zoroaster marambioensis*

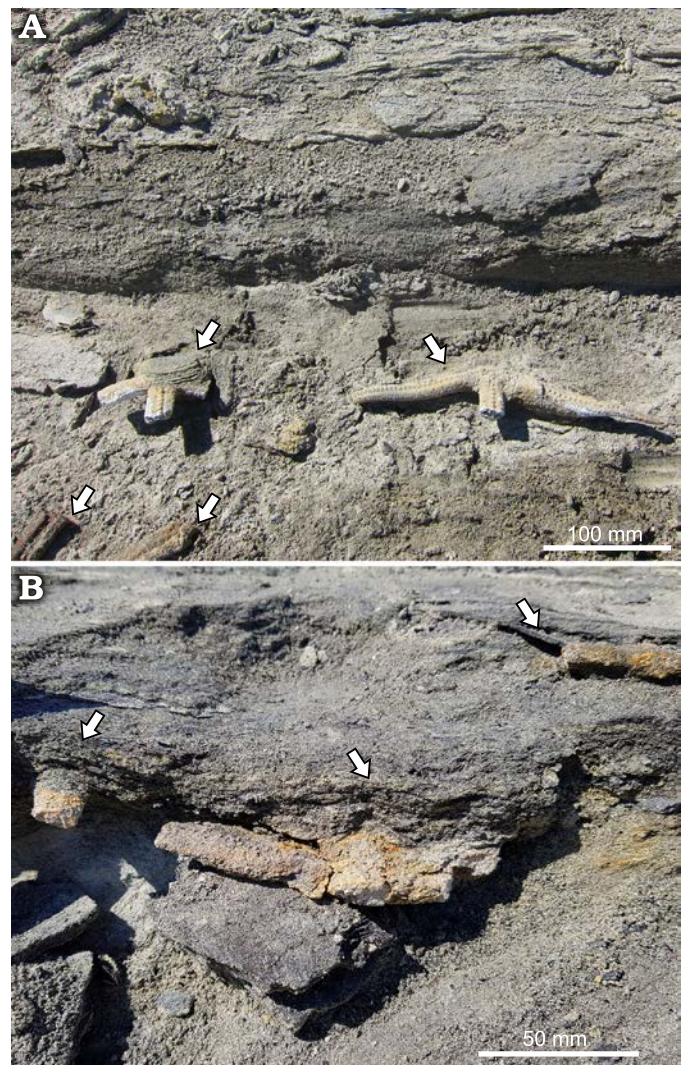


Fig. 3. Overview of asteroid layer in the type locality, GPS POI 64°14'24" S, 56°40'02" W, *Cucullaea* I Allomember, La Meseta Formation (Eocene). Seymour Island, Antarctica.

sp. nov. were also added to that matrix. Data was entered using Mesquite version 3.61 software (Maddison and Maddison 2019; SOM 1, Supplementary Online Material available at [http://app.pan.pl/SOM/app66-Palopolo\\_etal\\_SOM.pdf](http://app.pan.pl/SOM/app66-Palopolo_etal_SOM.pdf)) and exported to TNT version 1.5 (Goloboff and Catalano 2016) and PAUP trial version 4.0a167 (Swofford 2003). Analyses were performed following the methods of Mah (2007). Support estimation by Bootstrapping and Jackknifing methods were made using PAUP, with unrooted trees, unordered characters, 1000 replicates, gaps treated as “missing” and multi-state taxa interpreted as uncertainty. Bremer support was calculated using TNT software. Consistency and Retention indexes were calculated for consensus tree, bootstrapping and Jackknifing tree.

Terminology used for morphological characters follows previous descriptions (Hayashi 1943, 1961; Blake and Zinsmeister 1979, 1988; Blake and Aronson 1998; Blake 1987; Blake and Hotchkiss 2004; Mah 2007) and other publications about extant species (Mooi and David 2000; Sumida

et al. 2001; Howell et al. 2004; Mah and Blake 2012; Fau and Villier 2018). Systematic classification follows Spencer and Wright (1966), Blake (1987) and Mah (2007).

## Systematic palaeontology

Class Asteroidea Blainville, 1830

Superorder Forcipulatacea Blake, 1987

Order Forcipulatida Perrier, 1884

Family Zoroasteridae Sladen, 1889

Genus *Zoroaster* Thomson, 1873

*Type species*: *Zoroaster fulgens* Wyville Thomson, 1873; Eocene–Recent; Pacific, Atlantic and Indian oceans.

*Zoroaster marambioensis* sp. nov.

Figs. 4–9, SOM.

*Zoobank LSID*: urn:lsid:zoobank.org:act:A9C9FB9D-A846-48CD-A6A3-FB3B8B65A00E

1979 *Zoroaster* aff. *Z. fulgens* Thomson, 1873; Blake and Zinsmeister 1979: 1151–1152, pl. 2: 1–11.

1988 *Zoroaster* aff. *Z. fulgens* Thomson, 1873; Blake and Zinsmeister, 1988: 495, figs. 3: 7–10, 4: 1–4.

1998 *Zoroaster* aff. *Z. fulgens* Thomson, 1873; Blake and Aronson, 1998: 345.

*Etymology*: After the place of discovery, i.e., Marambio (Seymour) Island, Antarctic Peninsula.

*Type material*: Holotype: IAA-P-373-A, incomplete specimen comprising five fragments. Paratypes: IAA-P-373-B to K, ten incomplete specimens comprising four specimens with incomplete disc and arms, three specimens with complete disc and partially preserved arms, and three almost complete arm fragments without disc structures.

*Type locality*: GPS POI 64°14'24" S, 56°40'02" W, Seymour Island, Antarctica.

*Type horizon*: *Cucullaea* I Allomember, La Meseta Formation, Eocene.

*Material*.—Type material including holotype and ten incomplete specimens, one with complete disc and almost complete rays and the others with incomplete discs and arms; all of them preserved in detail, with spines, spinules and often pedicellariae. Twenty additional arm and disc fragments from the same stratum used for photographs and description. All from the same locality and layer.

*Diagnosis*.—Central disc plate enlarged, lobate, flattened or slightly depressed. Primary circlet with enlarged, lobate, tumid radials that abut small, polygonal and flattened inter-radials (Figs. 5A<sub>2</sub>, 7A, 9A<sub>3</sub>, B<sub>1</sub>, C<sub>2</sub>). Small abactinal disc plates between radials and central plate, and between primary circlet and marginals (Figs. 4A, B<sub>2</sub>, F<sub>2</sub>, 5A<sub>2</sub>, D). Primary spines on disc only present on radials. Marginals hexagonal, proximally with one spine every two marginals, distally lacking spines (Fig. 4A). Four or five rows of actinolaterals proximally, the upper row polygonal, without primary spines, extending distally until the area between the last two marginals at the arm tip (Figs. 5C<sub>3</sub>, 6A<sub>2</sub>, B<sub>1</sub>, B<sub>2</sub>, 8A<sub>1</sub>, A<sub>2</sub>). Oral armature well developed (Fig. 8B<sub>1</sub>, one to three spines for each prominent adambulacral and one

or two secondary spines). One or two big pedicellariae and 2–3 small pedicellariae associated to each prominent adambulacral plate (Fig. 6H<sub>1</sub>, H<sub>2</sub>). Each ambulacral plate with a long and well-developed furrow on actinal view (Figs. 4B<sub>1</sub>, H<sub>2</sub>, 6E). Terminals enlarged, crescent-shaped, wider than long, with a prominent notch (Fig. 8A<sub>1</sub>, A<sub>2</sub>). Primary spines short and blunt (on carinals) and long and slender (on actinolaterals). Secondary spines blunt on abactinal surface, sharp on actinal surface (see Table 1 for a succinct summary of the characters which distinguish this species from other zoroasterids).

*Description*.—Rays five. Major radius (R): 103–150 mm. Minor radius (r): 15–18 mm. R/r: 6.87–8.33. Breadth of the ray at its base: 13 mm. Eighteen marginals to first 10 carinals (Figs. 4F<sub>2</sub>, G<sub>1</sub>, H<sub>1</sub>, 9B<sub>1</sub>). Arms long, narrow, tapering distally (Fig. 4A, C<sub>1</sub>). Cross section of arms subcylindrical (Figs. 6B<sub>2</sub>, 7B, C). Entire body surface covered mainly by secondary spines (Fig. 4).

Disc small, tumid, interbrachial angles acute. Abactinal surface of the disc formed by a central ossicle, surrounded by a ring of five radials and five interradials, a madreporic plate, slightly modified marginals and a variable number of small abactinal disc ossicles (Figs. 5B<sub>1</sub>, 7A, 9B<sub>1</sub>). Centrale ossicle, when preserved, flattened or slightly depressed (the last character maybe as a taphonomic feature). Radials enlarged, tumid, weakly lobate, bearing a central primary spine, intercalated with smaller, flattened, polygonal interradials, covered by secondary spines (Figs. 5B<sub>1</sub>, 7A). Radials abut interradial ossicles (Fig. 9A<sub>3</sub>, C<sub>2</sub>). Madreporic plate relatively small (half the size of interradials), circular, slightly elevated, with multiple channels and pores radiating from the center (Figs. 4B<sub>2</sub>, 5E<sub>1</sub>, E<sub>2</sub>), not fused to the adjacent interradial ossicle (Fig. 7A), surrounded by secondary spines and pedicellariae, cup-shaped basal plates. Marginal plates on interbrachial angles enlarged, raised, subtriangular in shape, separated from the radials by small irregular inset adradial ossicles (Figs. 4A, B<sub>2</sub>, F<sub>2</sub>, 5A<sub>2</sub>, D). Disc ossicles articulated, leaving relatively large spaces for papulae.

Almost complete or fragmented arms articulated with the disc in most cases.

Arm plates articulated by proximal and distal lobes, relatively large spaces for papulae between plates at proximal part of the arms (Fig. 5C<sub>1</sub>, C<sub>4</sub>), becoming smaller distally. Ossicles arranged in well-defined longitudinal and transverse rows along arms (Figs. 5C<sub>1</sub>, C<sub>2</sub>, 9).

Carinals large, subcircular to hexagonal, weakly lobate (Fig. 5C<sub>4</sub>), transversely elongated proximally, equidimensional or slightly longitudinally elongated distally. Each carinal overlaps adjacent adradials and proximal carinal (Figs. 5C<sub>1</sub>, 9A<sub>3</sub>, C<sub>2</sub>). One big, short and blunt spine to each carinal, in a central knob of the ossicle (Figs. 4A, 6D, 7C).

Well-developed adradials in a single series along both sides of carinals, slightly depressed, covered by small secondary spines. Adradial ossicles hexagonal, almost equidimensional, sometimes transversely elongated (Figs. 5C<sub>1</sub>, 7B–D, 9A<sub>3</sub>, B<sub>1</sub>, C<sub>2</sub>), overlapped by carinals and marginals.



Table 1. Characters used in original descriptions to differentiate *Zoroaster* species. Abbreviations: ch., character; R, major radius (distance between the disc center and the arm tip); r, minor radius (distance between the disc center to the edge of the disc in the middle of an interradius); “?”, not stated in the original description; “–”, absent.

Characters	<i>Zoroaster actinocles</i> Fisher, 1919	<i>Zoroaster magnificus</i> Ludwig, 1905	<i>Zoroaster macracantha</i> H.L. Clark, 1916	<i>Zoroaster microporus</i> Fisher, 1916	<i>Zoroaster carinatus</i> Alcock, 1893	<i>Zoroaster fulgens</i> Wyville Thomson, 1873	<i>Zoroaster ophiactis</i> Fisher, 1916	<i>Zoroaster ophiurus</i> Fisher, 1905	<i>Zoroaster spinulosus</i> Fisher, 1906	<i>Zoroaster marambioensis</i> sp. nov.	
R	161	295	160	205	194	152	282	140	118	150	
r	11	14	14	12	13.5	31	15,5	10	11	18	
R/r	14.6	21.1	11.5	17	14	4.9	17	14	10.7	8.3	
Carinal primary spines	number	1	1	0	1 or more	1	1	1	1–3	1	
	shape	?	short, cylindrical	long (5 mm), sharp, pointed	–	similar to secondary spines	short, blunt	stout, cylindrical, long	thimble-shaped tubercle	short, conical, blunt	short, conical, blunt
Shape of secondary spines on abactinal surface	flesh, grooved	sharp, curved, grooved	short, blunt, grooved	?	thorn-like	thin, sharp	small, ungrooved	short (1mm), sharp, slender	short, delicate, papiliform	short, straight, sharp	
Pedicellariae on abactinal surface (ch. 71–72)	small, associated to poplar pores	big, straight	big, straight	?	few, small, scattered	?	small, associated with papulae	2–5, big, associated to carinals	–	small, associated to papulae	
Number of actinolateral rows (ch. 73)	3+1	4	3	?	?	5	6	5	5	5	
First row of actinolaterals different (ch. 74)	yes	yes	yes	?	?	yes	yes	yes	no	yes	
Actino-lateral primary spines	shape	slender	long, blunt, cylindrical	sharp, flattened	long, central	long, slender	long, flattened, sharp	sharp, flattened, long	sharp, slender, long	sharp, fine, delicate	sharp, flattened
	adpressed (ch. 75)	yes	yes	no	?	?	yes	yes	no	yes	yes
Actino-lateral pedicellariae	number (ch. 76)	1	?	several	?	?	?	?	1	several	0
	size (ch. 77)	big	?	small	?	?	?	?	big	small	–
Carinate adambulacrals	spine number	5	5	?	2	2–3	3–5	4–5	4–5	4	3
	pedicellariae above furrow (ch. 79)	small	big	?	?	?	big	big	big	big	big
	pedicellariae on innermost spine (ch. 78)	?	2–5	?	several	1 or 2?	5–8	10	6–8	5–8	2–3

Marginals in a single series (Figs. 4, 9), hexagonal, twice as wide as long, proximally bearing one primary spine every two marginals, distally without spines (Fig. 4A). Marginal series abutting adradials, but not actinolaterals (Figs. 5C<sub>2</sub>, 7B–D, 9A<sub>3</sub>, B<sub>1</sub>, C<sub>2</sub>).

Actinolaterals polygonal to subtriangular, arranged in 4–5 rows proximally, reduced to three on the distal half of the arm and becoming a single row near the arm tip (Figs. 5C<sub>2</sub>, C<sub>3</sub>, 7B–D, 9A<sub>1</sub>, A<sub>2</sub>). Upper row of actinolaterals smaller than marginals, equidimensional, alternated with marginals, without spines (Figs. 5C<sub>2</sub>, C<sub>3</sub>, 9A<sub>3</sub>). This series

does not articulate with the terminal ossicle, although the last actinolateral ossicle is located near the last distal marginal (Fig. 8A<sub>2</sub>). The three lower abactinal series bearing slender, elongated, usually flattened spines, directed upward and towards proximal part of arm, articulating with a central knob on each plate (Fig. 5C<sub>2</sub>, C<sub>3</sub>).

Adambulacrals plates alternating long carinate and short non-carinate ones (Figs. 4B<sub>1</sub>, D<sub>2</sub>, 6E, G, 9C<sub>3</sub>). Carinate adambulacrals bearing transverse series of stout cylindrical spines (Fig. 9A<sub>2</sub>, B<sub>2</sub>). Non-carinate adambulacrals at one side of the furrow is opposite to a carinate adambulacrals

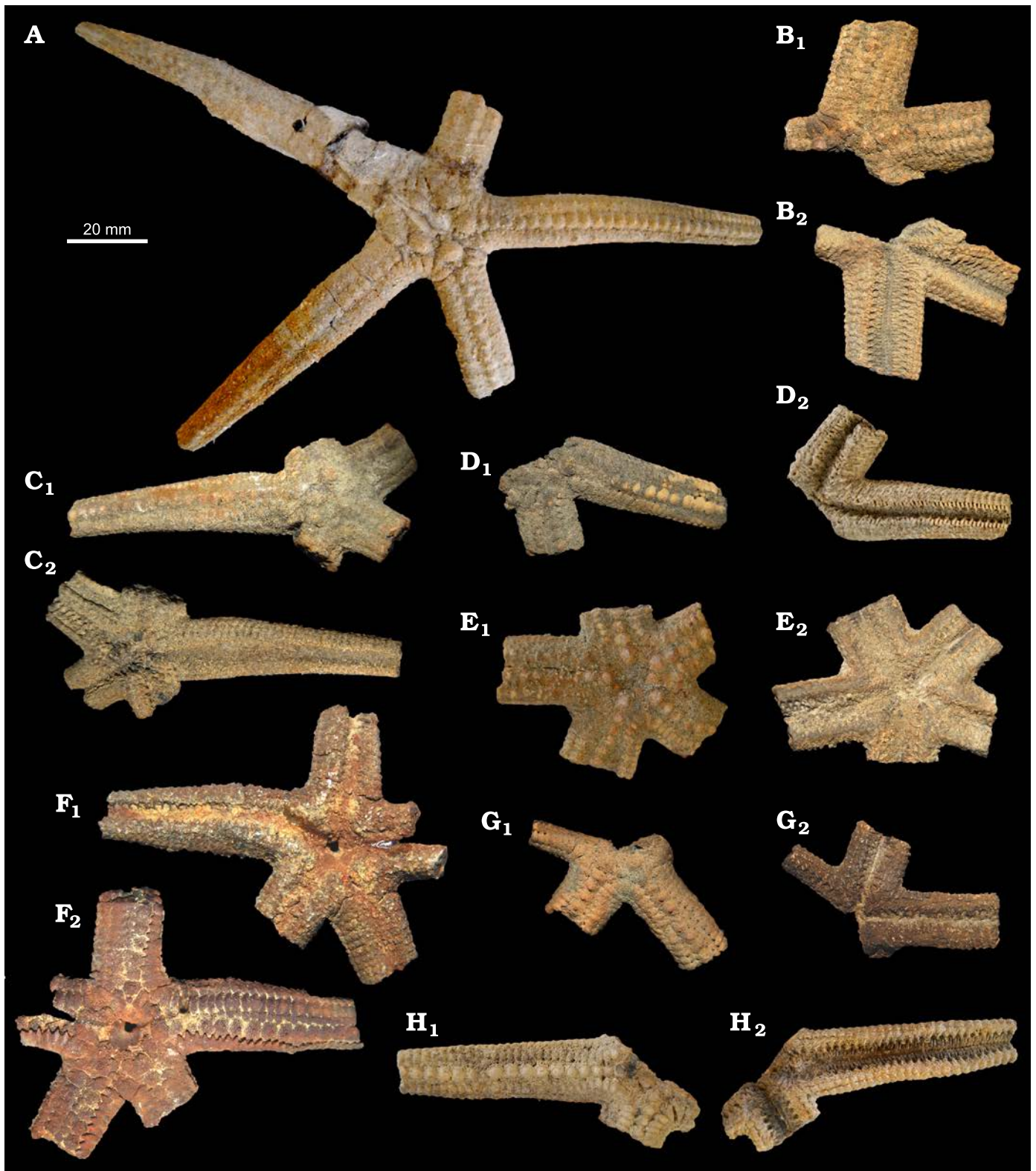


Fig. 4. Zoroasterid asteroid *Zoroaster marambioensis* sp. nov., Eocene, *Cucullaea* I Allomember, La Meseta Formation of Seymour Island, Antarctica. A. IAA-Pi-373-A, general view of abactinal surface. B–H. General appearance of each fragment in abactinal (B<sub>1</sub>–H<sub>1</sub>) and actinal (B<sub>2</sub>–H<sub>2</sub>) views. B. IAA-Pi-373-B. C. IAA-Pi-373-C. D. IAA-Pi-373-D. E. IAA-Pi-373-E. F. IAA-Pi-373-F. G. IAA-Pi-373-G. H. IAA-Pi-373-H.

on the other side (Fig. 9A<sub>1</sub>, B<sub>2</sub>). One to three spines for each prominent adambulacral, preserved in (or near) life position. One or two big pedicellariae (or cup-shaped basal piece),

two or three small pedicellariae, and one or two secondary spines (Figs. 6H<sub>1</sub>, H<sub>2</sub>, 9B<sub>2</sub>) associated to each prominent adambulacral.



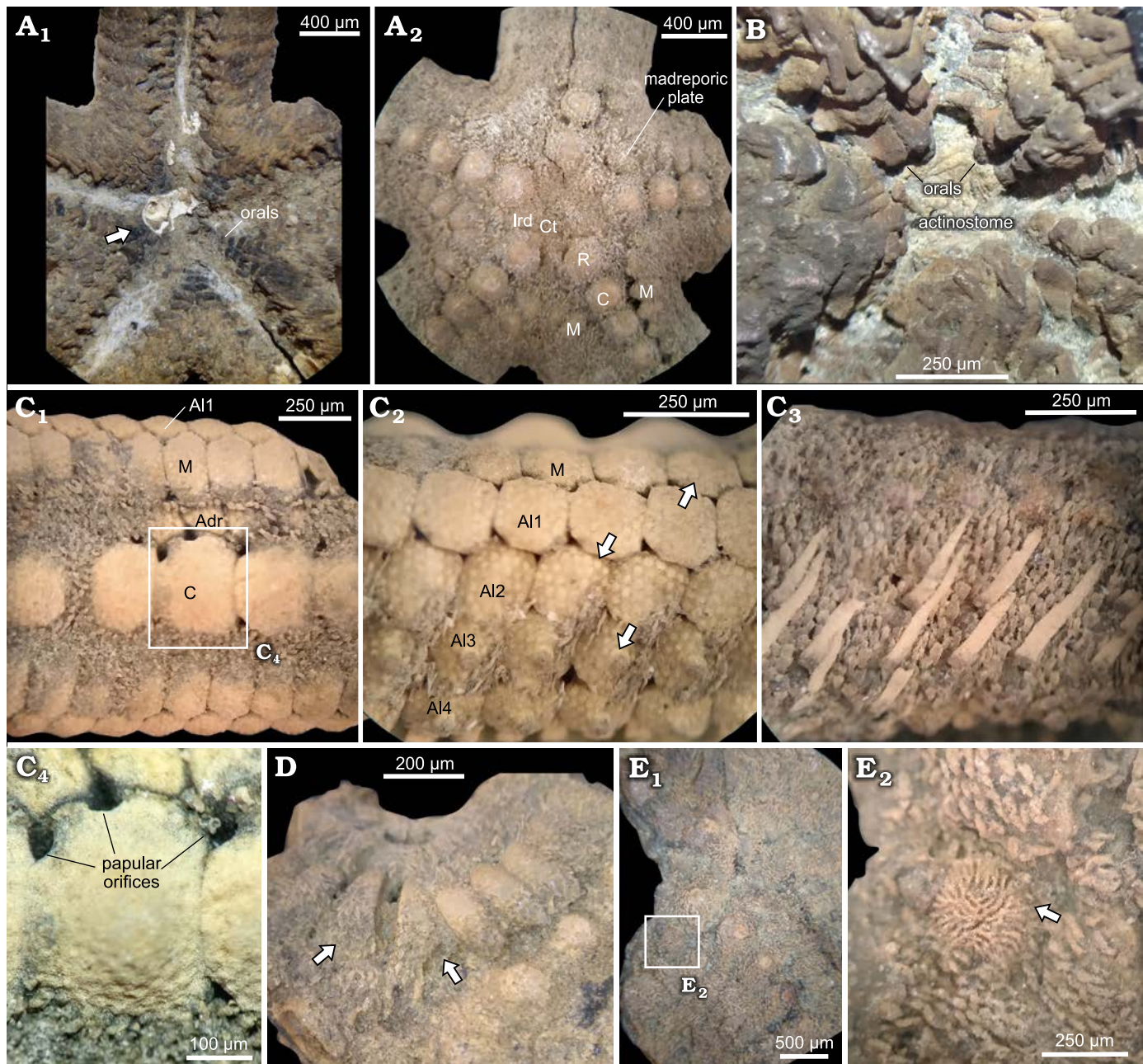


Fig. 5. Zoroasterid asteroid *Zoroaster marambioensis* sp. nov., Eocene, *Cucullaea* I Allomember, La Meseta Formation of Seymour Island, Antarctica. A. IAA-Pi-373-B, actinal (A<sub>1</sub>) and abactinal (A<sub>2</sub>) views. Gastropod valve near peristome location, partially attached to orals in actinal side (arrow). B. IAA-Pi-373-M, actinal view, showing oral depression, inferred position of actinostome and orals. C. IAA-Pi-373-E, detail of arm structures; abactinal view, indicating ossicle rows (C<sub>1</sub>); lateral view of distal, denuded part of the arm (C<sub>2</sub>), note the insertion marks left by primary and secondary spines on marginals and actinolaterals (arrows); lateral view of proximal part of arm, primary and secondary spine number and arrangement (C<sub>3</sub>); carinal ossicle structure and position of papular orifices (C<sub>4</sub>). D. IAA-Pi-373-I, interbranchial zone of disc on abactinal view, modified triangular marginals (arrows). E. IAA-Pi-373-C; position of madreporic plate on fragmented disc (E<sub>1</sub>); detailed structure of madreporite (arrow) (E<sub>2</sub>). Abbreviations: Adr, adradial; Al, actinolateral; C, carinal; Ct, central; Ird, interradial; M, marginal; R, radial.

Ambulacrals compressed, high, squarish-blocky in shape, directed towards the center of the ambulacral groove, with a long and well-developed furrow on actinal view (Figs. 4B<sub>1</sub>, H<sub>2</sub>, 6E, H<sub>1</sub>). Four rows of podial pores on actinal surface in the proximal part of the arm, becoming reduced to two series at the arm tip. Superambulacrals not observed, apparently reduced or absent.

Terminals, when preserved, highly enlarged, crescent-

shaped, wider than long (terminal length = 2/3 terminal width; Figs. 6B<sub>1</sub>, B<sub>2</sub>, 8A<sub>1</sub>, A<sub>2</sub>). Two lobes on abactinal surface of terminals articulated with last marginals, last carinal on prominent notch of terminals (Fig. 8A<sub>1</sub>). On actinal view, terminals have an oval depression, where the last pair of distal ambulacral and adambulacral ossicles are articulated (Fig. 8A<sub>2</sub>). Stereom of terminal plate well preserved on actinal side (with smooth and regular



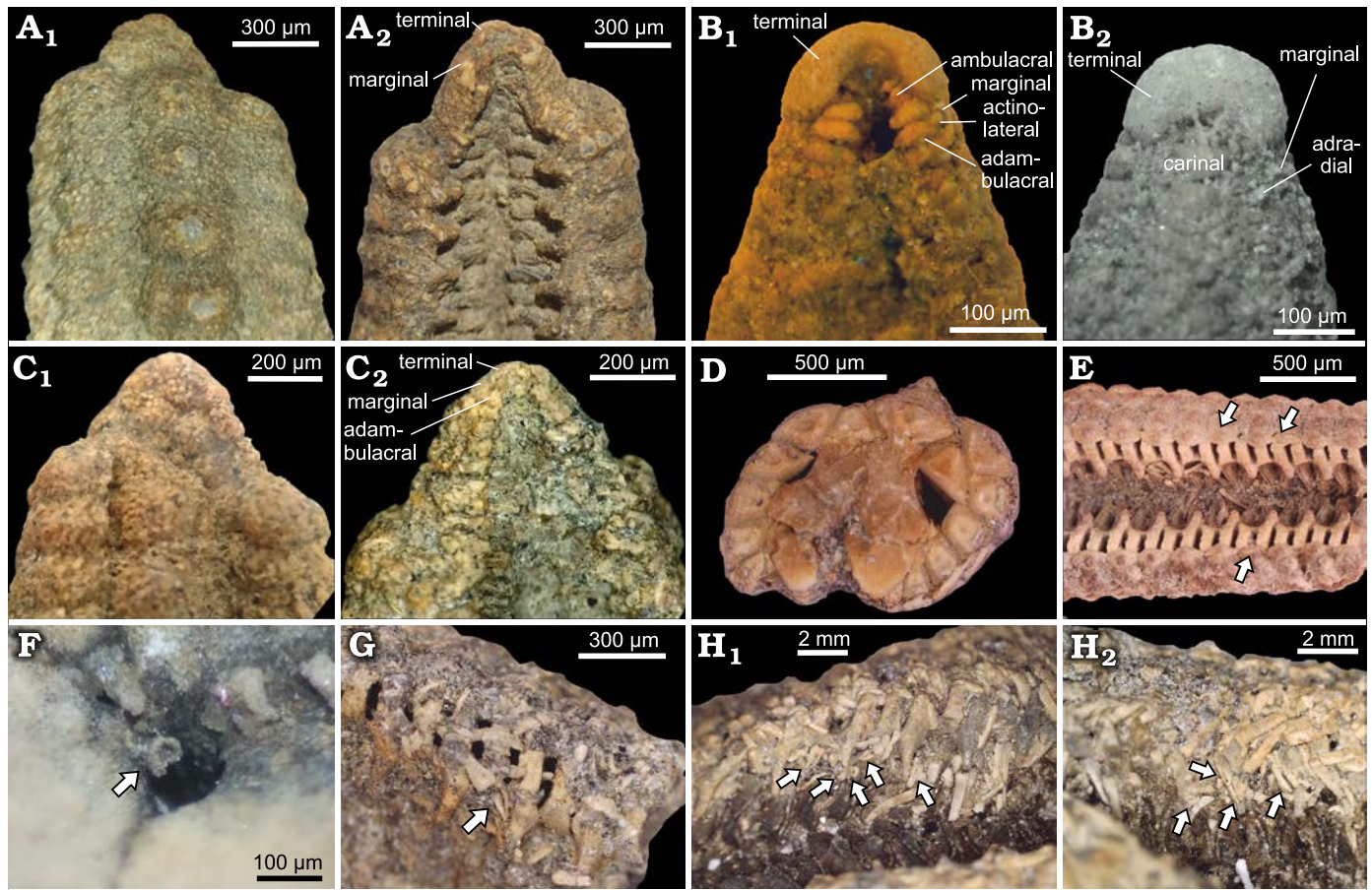


Fig. 6. Zoroasterid asteroid *Zoroaster marambioensis* sp. nov., Eocene, *Cucullaea* I Allomember, La Meseta Formation of Seymour Island, Antarctica. A. IAA-Pi-373-K, abactinal (A<sub>1</sub>) and actinal (A<sub>2</sub>) views of a regenerating arm tip, note the size differences between ossicles and terminal small and inconspicuous. B. IAA-Pi-373-N, abactinal (B<sub>1</sub>) and actinal (B<sub>2</sub>) views of arm tip. C. IAA-Pi-373-L, regenerating arm tip on abactinal (C<sub>1</sub>) and actinal (C<sub>2</sub>) views, note small ossicles in chaotic arrangement on abactinal side. D. IAA-Pi-373-Q1, transverse section of a partially deformed ray. E. IAA-Pi-373-Q4, actinal view of a ray on the second third section, note that the third row of actinolaterals is reduced towards the arm tip (arrows). F. IAA-Pi-373-E, close-up of popular pore with small pedicellariae basal plate (arrow). G. IAA-Pi-373-E, small pedicellariae blades (arrow) on associated to a non-carinate adambulacral (arrow). H. IAA-Pi-373-R, inclined views of arms in life position; furrow with two big and three small pedicellariae (arrows) (H<sub>1</sub>); arm with three big pedicellariae (arrows) (H<sub>2</sub>).

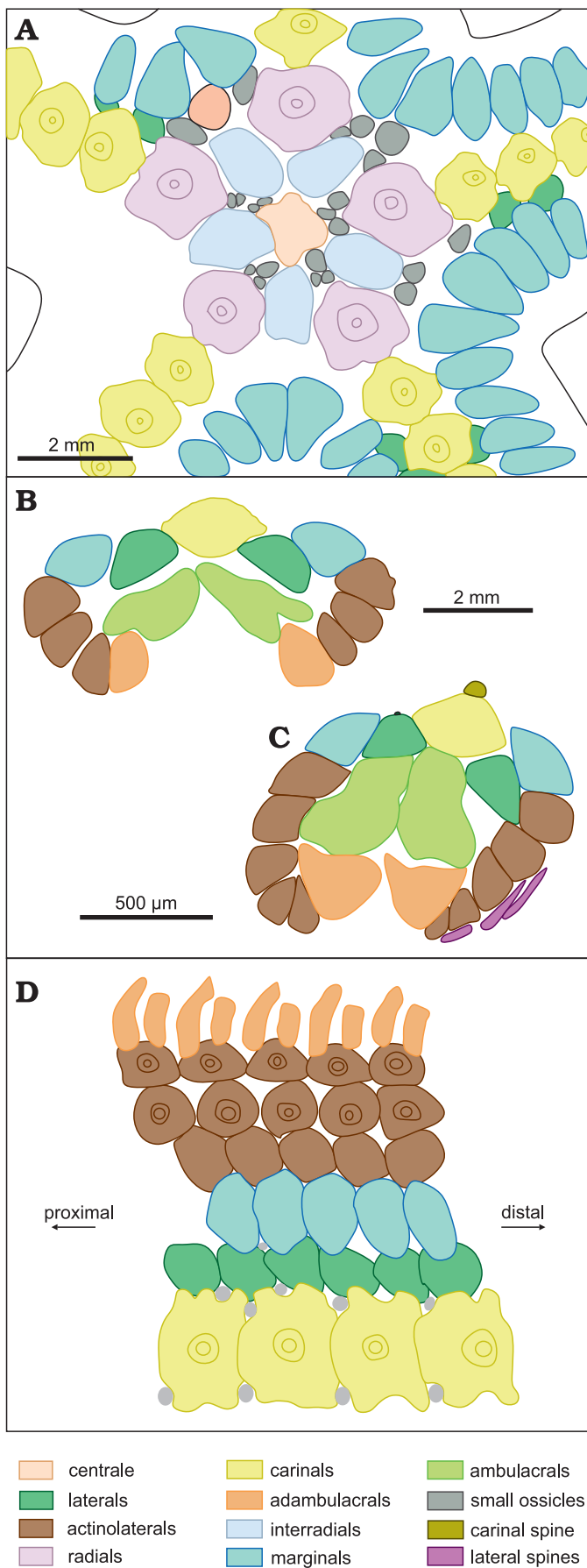
calcitic trabeculae), altered and pitted on abactinal side (Fig. 8A<sub>3</sub>, A<sub>4</sub>).

Primary and secondary spines attached in life position in adambulacrals, actinolaterals, marginals, and carinal ossicles, with massive spine bases. Secondary spines arranged in groups around the carinal spine bases, closely spaced in other plates of actinal and abactinal surface. When not preserved, secondary spine position is inferred by circular marks on the ossicles (Figs. 4D<sub>1</sub>, F<sub>2</sub>, G<sub>1</sub>, H<sub>1</sub>, 5C<sub>1</sub>, C<sub>2</sub>). There are two types of secondary spines; those on the actinal surface are slender and longer than those on the abactinal surface (Figs. 4F<sub>2</sub>, G<sub>1</sub>, 6G, H<sub>1</sub>, H<sub>2</sub>). Pedicellariae straight, 200–600 µm long, formed by two blades and a cup-shaped basal piece. Pedicellariae significantly more abundant on actinal surface than in abactinal surface, inferred by the presence of complete pedicellariae and basal pieces without attached blades on both actinal and abactinal surfaces.

Actinal surface of disc preserved in detail. Actinostome deeply sunken, in a central depression (Figs. 5B<sub>2</sub>, 9B<sub>2</sub>). Oral

area delimited by one pair of adambulacrals from each arm, articulated with small orals (Figs. 5A, B<sub>2</sub>, 9B<sub>2</sub>). Each oral ossicle bearing oral spines (Fig. 9A<sub>4</sub>).

*Remarks.*—Studied specimens are assigned to *Zoroaster* because of disc characters (i.e., weakly lobate disc plates, disc and arm plates continuous, see Figs. 4A, 5A<sub>2</sub>, 7A, 8B<sub>2</sub>), imbricate ossicle arrangement (Figs. 4, 9), the presence of plates aligned in transverse and longitudinal series (Figs. 5C, 9A<sub>1</sub>–A<sub>3</sub>), consistently sized marginals (Figs. 4A, 7D, 9B<sub>1</sub>), secondary spines widely spaced in actinal and abactinal surface (Figs. 5, 6H), carinate adambulacral plates alternating with non-carinate plates (Fig. 6E) and podial pores quadriseriate proximally, becoming biserial distally. Within the imbricate Zoroasteridae, *Bythiolopus* Fisher, 1916, *Doraster* Downey, 1970, and *Cnemidaster* Sladen, 1889, have internal buttress and a ring of oral pedicellariae, while these structures are absent in *Zoroaster* and *Pholidaster* Sladen, 1889. Also, *Bythiolopus* and *Pholidaster* have alternated big and small marginal plates, while in



*Zoroaster* marginals are consistently sized. *Cnemidaster* has enlarged, rounded and swollen disc plates, and discontinuous disc and arm plates. *Doraster* has a similar disc plate arrangement, but differs from *Cnemidaster* in having highly stellated disc plates. *Zoroaster* has weakly lobated disc plates, similar in size with the arm plates. The body wall in *Cnemidaster* is covered by membranous skin, while in *Zoroaster* is covered by secondary spines, that are frequently absent in *Doraster* and *Pholidaster*. Straight pedicellariae are absent in *Pholidaster* but present in *Zoroaster*.

*Zoroaster marambioensis* sp. nov. has the same number of actinolateral rows as *Zoroaster microporus* Fisher, 1916, but the former has spines only in the three or four actinolateral lower rows while the latter has primary spines in all actinolaterals. Also, *Z. microporus* lacks primary spines on carinals and marginals, while *Z. marambioensis* sp. nov. has primary spines on each carinal, and on some proximal marginals. The carinal plates of *Z. marambioensis* sp. nov. are weakly lobate, as in all the other species of the genus, except *Z. microporus*, which has quadrate carinals. *Zoroaster marambioensis* sp. nov. has quadriserial arrangement of podial pores proximally, while *Z. microporus* and *Zoroaster ophiactis* Fisher, 1916, have a biserial tube feet arrangement.

*Zoroaster carinatus* Alcock, 1893, differs from Antarctic species by showing a centrally domed disc, disc plates without secondary spines, lack of carinal and marginal spines along arms, and quadriserial tube feet along almost all of the rays.

*Zoroaster marambioensis* sp. nov. is similar to *Zoroaster variacanthus* McKnight, 2006, in having four or five rows of actinolaterals at arm base reduced to three or two at proximal half of the arm (the lower three with a large and usually flattened spine), plates densely covered by secondary spines partially obscuring ossicle outlines, and rare pedicellariae in abactinal surface. Nevertheless, *Z. variacanthus* has longer than wide carinal plates, inconspicuous madreporite, more than one spine on disc plates, and spines in each marginal plate.

*Zoroaster marambioensis* sp. nov. differs from *Zoroaster fulgens* Thomson, 1873, in having a flattened or slightly depressed central disc plate (Fig. 9B<sub>1</sub>, C<sub>2</sub>); weakly lobate radials overlapping polygonal interradials on the disc circlet (Figs. 4B<sub>2</sub>, 5A<sub>2</sub>, 9A<sub>3</sub>, B<sub>1</sub>, C<sub>2</sub>); marginal plates hexagonal or polygonal in shape lacking spines distally (Figs. 4A, D<sub>1</sub>, G<sub>1</sub>, 5C; 7B–C, 9B<sub>1</sub>); but with spines present on all carinals and radials (Figs. 4B<sub>2</sub>, H<sub>1</sub>, 6A<sub>2</sub>, D, 7C; note that in *Z. fulgens* primary carinal spines are absent and radials and interradial plates of disc have the same shape). *Z. marambioensis* sp.

Fig. 7. Diagrams of plate arrangement on disc and arms of zoroasterid asteroid *Zoroaster marambioensis* sp. nov., Eocene, *Cucullaea* I Allomember, La Meseta Formation of Seymour Island, Antarctica. Note the presence of a single row of marginal ossicles. A. IAA-Pi-373-B, abactinal view of disc. B. IAA-Pi-373-H, transverse section of arm. C. IAA-Pi-373-Q1, transverse section of a partially deformed ray. D. Shape and arrangement of all the ossicle rows of an arm, projected on a plane. D not to scale.



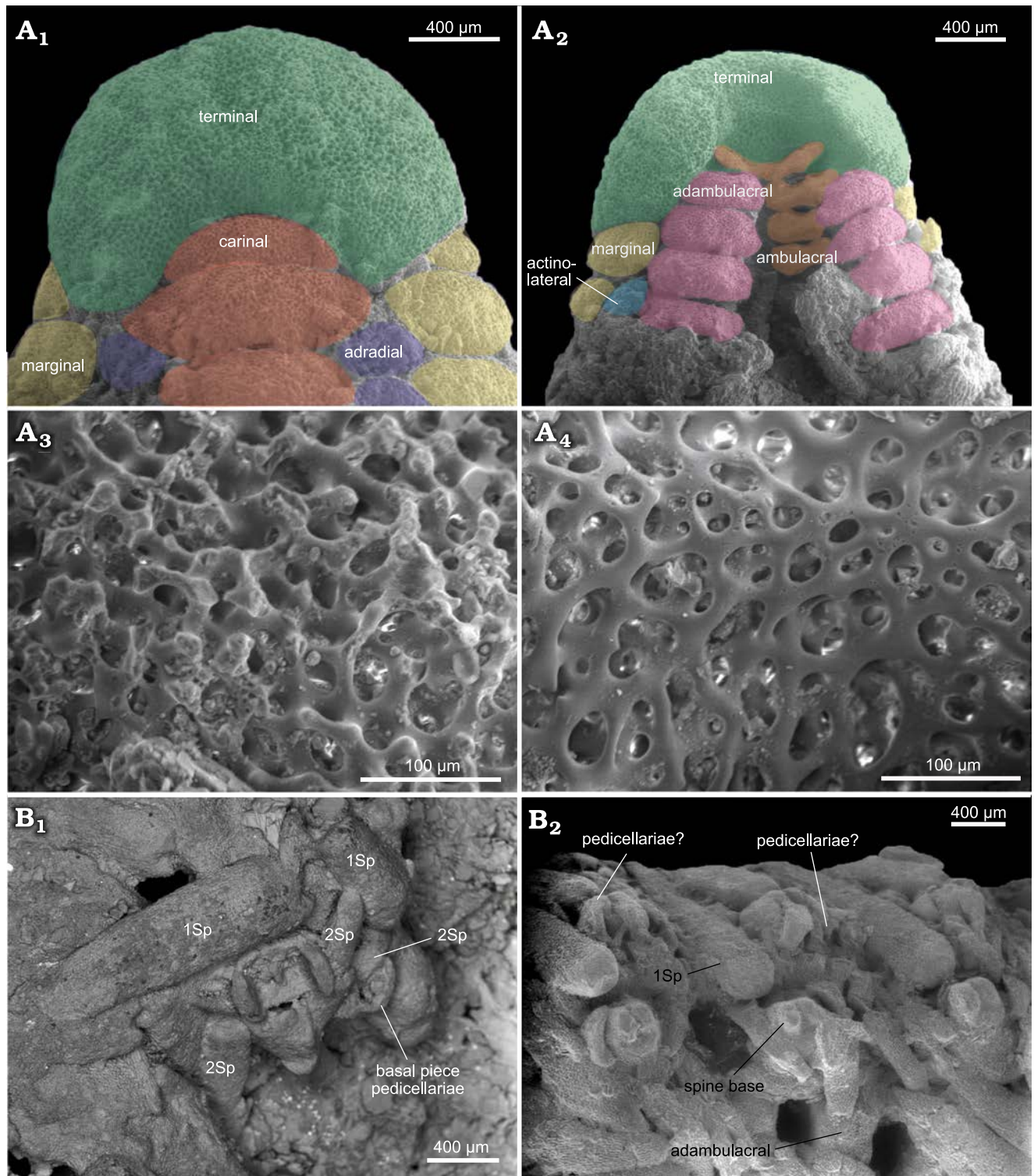


Fig. 8. Zoroasterid asteroid *Zoroaster marambioensis* sp. nov., Eocene, *Cucullaea* I Allomember, La Meseta Formation of Seymour Island, Antarctica. **A.** IAA-Pi-373-N, arm tip, detailed abactinal (A<sub>1</sub>) and actinal (A<sub>2</sub>) views of distal and terminal ossicles; detailed stereom structure of terminal ossicle in abactinal (A<sub>3</sub>) and actinal (A<sub>4</sub>) surface, note that the fossil was preserved in life position, then the stereom in abactinal surface was unaltered. **B.** IAA-Pi-373-G; position and arrangement of primary and secondary spines and pedicellariae in actinal inclined side of arm (B<sub>1</sub>); lateral view of arm, showing spines and pedicellariae associated to actinolaterals (B<sub>2</sub>). Abbreviations: 1Sp, primary spine; 2Sp, secondary spine.

nov. has wider than long terminal ossicle, with a prominent notch (Figs. 6B<sub>1</sub>, B<sub>2</sub>, 8A<sub>1</sub>, A<sub>2</sub>), while terminal plates on *Z. fulgens* are longer than wide and have reduced notch. Also, their primary and secondary spine arrangement on

the actinal surface is different (*Z. fulgens* has two primary spines and three secondary spines by each carinate adambulacral, while *Z. marambioensis* sp. nov. has one to three primary spines and one or two secondary spines by each

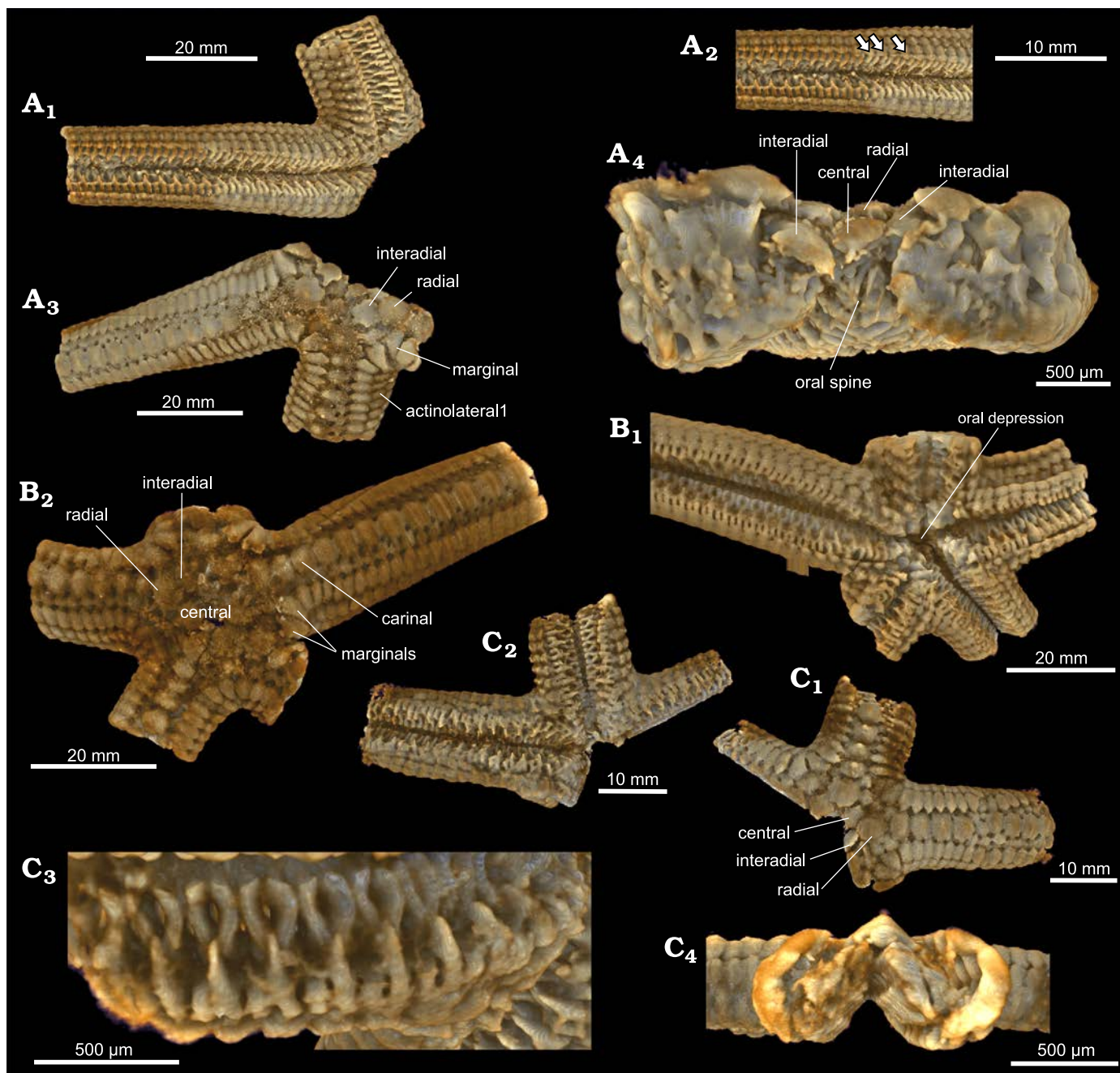


Fig. 9. Zoroasterid asteroid *Zoroaster marambioensis* sp. nov., Eocene, *Cucullaea* I Allomember, La Meseta Formation of Seymour Island, Antarctica. Volume rendering captions from microCT (SOM 2). A. IAA-Pi-373-E; general actinal surface reconstruction (A<sub>1</sub>); detailed arm structure on actinal side (A<sub>2</sub>), see primary and secondary spines preserved in detail and last ossicles of 4th actinolateral row (arrows). general abactinal surface reconstruction (A<sub>3</sub>) transverse view of disc structures, see orals and oral spines on disc center (A<sub>4</sub>). B. IAA-Pi-373-D, general reconstructions of abactinal (B<sub>1</sub>) and actinal (B<sub>2</sub>) surfaces. C. IAA-Pi-373-G; reconstructions of abactinal (C<sub>1</sub>) and actinal (C<sub>2</sub>) surfaces; structure detail on inclined side of arm (C<sub>3</sub>); transverse section of a ray (C<sub>4</sub>).

adambulacral; see Figs. 6G, H<sub>1</sub>, H<sub>2</sub>, 8B<sub>1</sub>, B<sub>2</sub>). In *Z. marambioensis* sp. nov. the adradials and the last row of actinolaterals extends until most distal part of the arm, near the terminal ossicle, separated from it only for the last marginal plate (Figs. 6A<sub>1</sub>–C<sub>2</sub>, 8A<sub>1</sub>, A<sub>2</sub>), while in *Z. fulgens* the last adradial and actinolateral plates are aligned with the fourth or fifth marginal plate (counting from the arm tip). This actinolateral row arrangement is closer to those described by

Ludwig (1905) for *Zoroaster magnificus* than the observed in *Z. fulgens* specimens.

As described by Howell et al. (2004), Recent *Z. fulgens* from the Atlantic Ocean appears as three morphotypes that could show reproductive isolation: the robust morphotype, the slender form and the long-armed one, which inhabit at depths of 975–1750 m, 1300–2200 m, and 3300–4020 m, respectively. This suggests that cryptic species are pres-



ent across the bathymetric range of this species. *Zoroaster marambioensis* sp. nov. shows many similarities with the robust morphotype of *Z. fulgens* in characters typically associated with shallower environments (i.e., solid skeletons, short arms and strong oral armature), although the former were found in beds deposited at 10–20 m depth and the latter inhabits (at least) at 200 m depth.

In addition to *Zoroaster marambioensis*, described herein from Seymour Island, only one other Eocene fossil *Zoroaster* species is known, i.e., *Zoroaster whangareiensis* Eagle, 2006, from New Zealand. Despite the poor preservation of *Z. whangareiensis*, several differences with *Z. marambioensis* sp. nov. are recognizable. *Z. whangareiensis* has carinal spines placed proximally after the 4th or 5th carinal, and distally every second carinal; enlarged, central, single, conical spines every second marginal and 5–6 small spinules for each marginal. *Z. marambioensis* sp. nov. is larger than *Z. whangareiensis* and has a more robust armature. Madreporite, terminal ossicles, pedicellariae, secondary spines, ambulacral armature, spine number, size and arrangement on oral surface are unknown characters in *Z. whangareiensis*.

*Stratigraphic and geographic range.*—Type locality and horizon only.

## Systematic and phylogenetic analyses

Mah (2007) published an extensive revision of the family Zoroasteridae. Although the author did not attempt a review of the genus *Zoroaster*, he found that resolution within the *Zoroaster* clade is poor, only moderately supporting the clades *Zoroaster carinatus* and *Zoroaster fulgens*, and grouping the other seven species in a single clade (*Zoroaster actinocles* Fisher, 1919, *Zoroaster macracantha* Clark, 1916, *Zoroaster magnificus* Ludwig, 1905, *Zoroaster ophiactis* Fisher, 1916, *Zoroaster ophiurus* Fisher, 1905, *Zoroaster spinulosus* Fisher, 1906, and *Zoroaster* aff. *Z. fulgens* Blake and Zinsmeister, 1979), with few to no character differences (Mah 2007).

According to the descriptions of species of *Zoroaster*, it seems likely that the diagnostic characters within the genus could be (i) type of primary and secondary spines (combining shape and size), (ii) actinal armature configuration (including number of primary and secondary spines associated with prominent adambulacral plates; number, shape and size of pedicellariae within the actinal area; number of spines that are directed into the furrow; etc.), (iii) number of

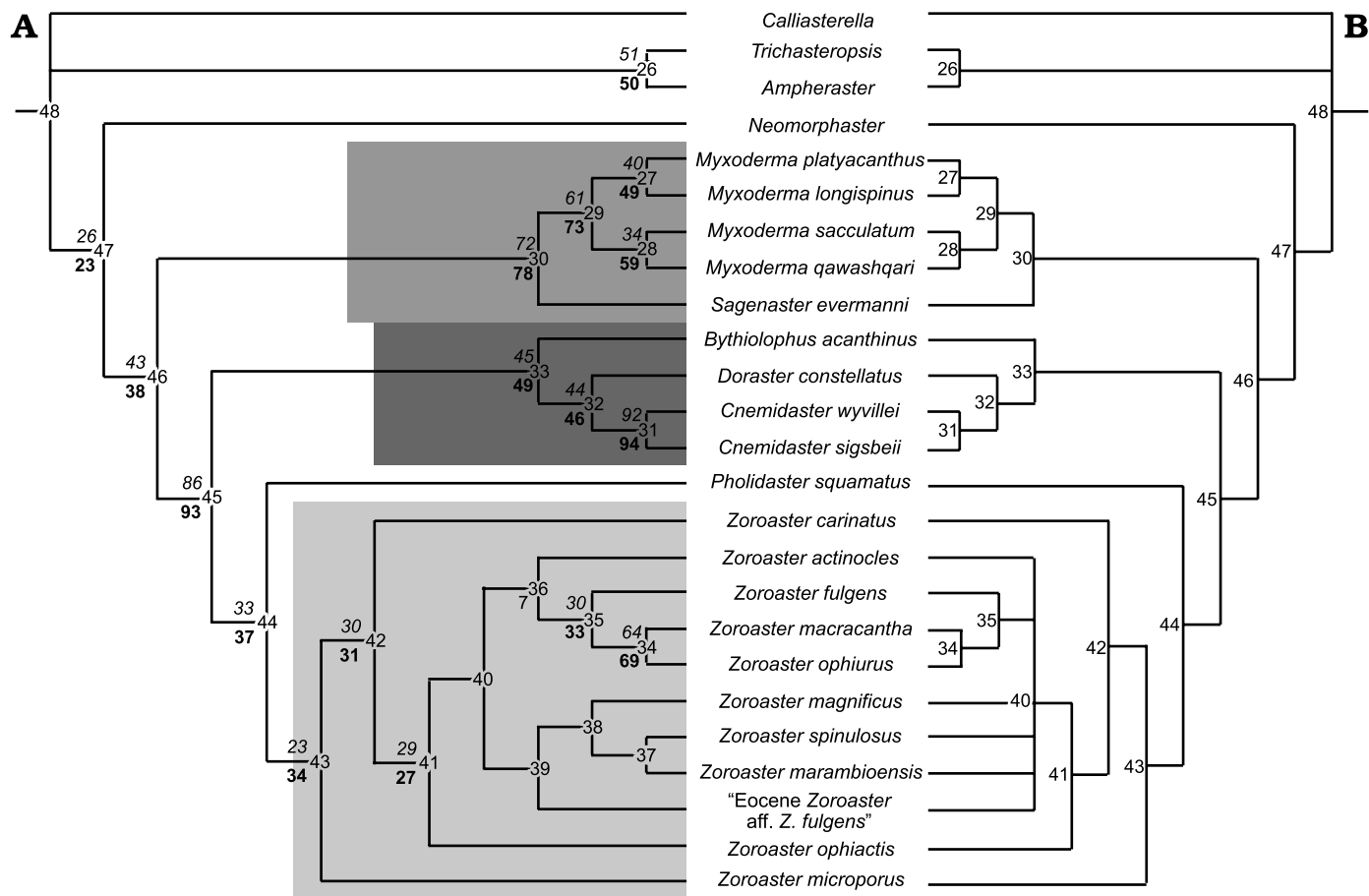


Fig. 10. Most parsimonious (A) and consensus (B) tree from the Zoroasteridae. Bootstrap values are in boldface below and Jackknife values are shown in italics to the left above the node numbers in the cladogram.

actinolateral plate series, and (iv) spine distribution within abactinal and lateral plate series.

We carefully re-evaluated the matrix published by Mah (2007) and found out that some characters in this matrix seem to be inconsistent. Character 1.21 is a presence-absence character (0–1), but it is coded “2” for *C. wyvillei* and *C. sigsbeii*. Character Group 3 has some problems too, i.e., *Calliasterella* species do not have actinal or actinolateral plates, as stated by Mah (2007) in character 3.1. Characters 3.2–3.6 refer to distribution, orientation, and spinulation of such ossicle type and are coded in *Calliasterella* as absent (3.1, 3.2, 3.3, and 3.5) and imbricate (3.4), perhaps meaning lack of orientation, spines, and density instead of ossicle absence. Finally, soft tissue characters (5.1 and 5.2) are coded as absent for Eocene *Zoroaster* aff. *Z. fulgens* Blake and Zinsmeister, 1979, but Blake and Zinsmeister (1979) did not mention the presence of soft parts and thus the states of these characters cannot be assumed as present or absent in fossils. It remains unclear then how these could be presence/absence characters in the Eocene species. Despite these observations, *Z. marambioensis* sp. nov. characters were added to the previous matrix without previously modifying it, i.e., we used the original matrix published by Mah (2007).

Nine characters were added to the matrix of Mah (2007) (Appendix 1, SOM). A Heuristic Search with PAUP and TNT software returned 7 most parsimonious trees with a tree length of 172. Values of Consistency Index, Homoplasy Index and Retention Index were 0.6395, 0.3605, and 0.7989, respectively. Consensus tree is displayed in Fig 10.

This consensus tree rendered a basal group within the class Asteroidea including *Calliasterella*, *Trichasteropsis*, and *Ampheraster* (node 26) and *Neomorphaster*. The latter remains as sister group of all the *Zoroasteridae* clade. The group including species of *Myxoderma* and *Sagenaster* (node 30) is well separated from the rest of the *Zoroasterid* species. Thus, “reticulated” and “imbricated” *Zoroasterids* are clearly differentiated (as established by Mah 2007).

A third well-supported group is the clade “*Cnemidaster* + *Doraster* + *Bythiolopus*” (node 33). It is supported by characters 19 (1.19), 44 (3.10), 66 (8.8) and 74.

The genera *Zoroaster* and *Pholidaster* are grouped together (node 43), with *Pholidaster* as sister group of *Zoroaster*. *Zoroaster microporus* remains basal to all species of *Zoroaster* (node 42). Within the other *Zoroaster* species, *Z. actinocles*, *Z. fulgens*, *Z. macracantha*, and *Z. ophiurus* (node 36) are recovered as sister group of *Z. marambioensis* sp. nov., Eocene *Zoroaster* aff. *Z. fulgens* Blake and Zinsmeister, 1979, *Z. magnificus*, and *Z. spinulosus* (node 39). Node 36 is supported by characters 76 and 77, while node 39 is supported only by character 78. Within node 39, *Z. marambioensis* sp. nov. is supported by characters 16 (1.16), 17 (1.17), and 65 (8.7).

The Bootstrap and Jackknife values show (within the *Zoroaster* species) a strongly supported group including *Z. macracantha* and *Z. ophiurus*. The clade *Z. fulgens*–*Z. macracantha* + *Z. ophiurus* is moderately to poorly sup-

ported, but is recovered in all the most parsimonious trees as separated from the other *Zoroaster* species.

## Concluding remarks

All evidence suggests that the layer yielding the fossil material studied represents an autochthonous simple episodic deposition event (Kidwell 1991), where starfishes were simultaneously killed and buried by a rapid event. The fossil assemblage could be assigned to taphofacies IIA, as they are concentrated in a particular 3–5 cm thick bed, well-calcified, showing little or no breakage and minor to no abrasion, corrosion, or bioerosion (Brett et al. 1997). *Zoroasterids* colonized a distal part of an estuary under normal marine salinity and were killed by the input of freshwater carried by a hyperpycnal flow, and immediately buried by fine grained sand from suspension clouds related to the buoyant inversion of hyperpycnal flows at flow margin areas.

Preservation of labile structures (i.e., primary and secondary spines, and pedicellariae basal plates with or without articulated blades; Fig. 6I–L) helped to assess possible hypotheses regarding the studied material. Straight pedicellariae and cup-shaped basal plates were observed in our specimens, which are closely similar to those found in the extant species of the genus. Results seem to show that characters of pedicellariae did not change since the Eocene.

Phylogenetic results support the “reticulate” and “imbricate” *Zoroasteridae* identified by Mah (2007). The former includes *Myxoderma* and *Sagenaster*, while the latter comprises *Bythiolopus*, *Doraster*, *Cnemidaster*, *Pholidaster*, and *Zoroaster*. The characters added to the matrix slightly changed the cladogram. *Zoroaster microporus* was retained as basal within the *Zoroaster* species, then *Z. carinatus* was identified as basal to a cluster of nine species. The cluster including *Z. fulgens*, *Z. macracantha*, and *Z. ophiurus* is recovered in all trees, supported by characters 71 (pedicellariae associated to carinal ossicles), 72 (big pedicellariae on abactinal surface), 73 (five actinolateral rows) and 78 (5–8 pedicellariae on innermost spine of carinate adambulacra).

Fifteen characters code differently for *Z. fulgens*, Eocene *Zoroaster* aff. *Z. fulgens* Blake and Zinsmeister, 1979, and *Z. marambioensis* sp. nov. Among these, seven characters cannot be observed in the studied specimens of *Z. marambioensis* sp. nov. as they were all related to soft tissue or superambulacral features.

The material studied herein are remarkably similar to those of the Eocene *Z. aff. Z. fulgens* from Seymour Island. A more detailed review of certain characters not recognizable in the specimens studied by Blake and Zinsmeister (1979) allowed improving the description of the species and clearly differentiate the specimens found in Seymour Island from *Z. fulgens*.

The addition of characters to the matrix published by Mah (2007) reveals that a profound revision of *Zoroaster* is needed to clearly establish which are the key characters to



identify species within this genus. Future research should include morphological characters related to the “ambulacral armature” and the “disc plate arrangement” as well as molecular data (for extant species). Molecular characters could prove a higher resolution than morphological characters, considering that Howell et al. (2004) stated that the gene flux and reproductive isolation of the morphotypes of *Z. fulgens* could indicate a depth-controlled speciation.

Some fossil zoroasterids appear in locations and environments different from those where extant members of the family live, although this could be due to an artefact of depositional environment. Eocene zoroasterids were epifaunal, inhabited shallow environments in the proximal platform, and coexisted with several groups of predatory and scavenger organisms (Blake and Zinsmeister 1979). Recent species of *Zoroaster* live in deep water, where predator pressure is lower than in shallow marine environments (Downey 1970; Howell et al. 2004; Mah, 2007; Aronson et al. 2009).

Meyer and Oji (1993) suggested that predation pressure and temperature are very important factors that could control the presence of echinoderms in Eocene nearshore environments in the Antarctic continent. Teleosts and other predators (including sea urchins) generated selection pressure on the crinoids causing their migration into deeper waters (Aronson et al. 1997, 2009). In fact, Gorzelak et al. (2012) concluded that benthic predation by sea urchins was an important, if not the main, causal driver of biological change throughout the Mesozoic, and that it may have set the stage for the recent pattern in which motile crinoids greatly predominate over sessile forms that live only at great depths. Like crinoids, stelleroids and the studied material shows no significant signals of damage caused by predation (Blake and Zinsmeister 1979, 1988; Baumiller and Gaździcki 1996; Aronson et al. 1997; this publication), except for two fragments of possible regenerated arms of *Zoroaster marambioensis* sp. nov. (Fig. 6A, B, E, F). Also, teleost fishes, which prey upon asteroids, are poorly represented in La Meseta Formation (Clarke and Johnston 2003). Therefore, it could be possible that these factors aided in the survival of those echinoderm groups in shallow water environments until the late Eocene. The discovery of new strata with echinoderm concentrations in the La Meseta Formation could reinforce the anomaly defined by Aronson et al. (1997) as “anachronistic, Paleozoic-type, low-predation communities”, where echinoderms were dominant and show almost non-existent damage and regeneration rates. Whittle et al. (2018), however, argued that benthic marine faunas from South America, Antarctica, Australia and New Zealand had the same community structure with a continuous record of shallow marine stalked crinoids from the Cretaceous to the Paleogene, without signs of reversions. They also stated that subsequent changes in benthic faunal composition could have been driven either by increasing predation pressure or, more likely, by competition with other echinoderm groups (such as comatulid crinoids).

The Antarctic continent experimented great climatic changes since the middle Eocene. During the Paleogene, surface water temperature was stable between 10–15°C (Zinsmeister 1982; Meyer and Oji 1993). Several studies using  $\delta^{18}\text{O}$  (Gaździcki et al. 1992; Aronson and Blake 2001; Dutton et al. 2002 and references therein; Ivany et al. 2008) and, recently, multiproxy data including  $\text{TEX}^{\text{L}}_{86}$  calibration of surface sea temperatures (Douglas et al. 2014) agree that there was an increase in high latitude surface sea temperature during the early Eocene, with a climatic optimum in the middle Eocene. Surface sea temperatures at the Middle Eocene Climate Optimum were estimated in 10–17°C using  $\delta^{18}\text{O}$  (Douglas et al. 2014) and in 24°C with  $\text{TEX}^{\text{L}}_{86}$  calibration (Bijl et al. 2013). After that there was a sharp cooling caused by the opening of the Drake Passage and the development of the Antarctic Circumpolar Current, with a 7–9°C drop in sea water temperatures at the Eocene/Oligocene boundary (Aronson et al. 1997; Aronson and Blake 2001; Ivany et al. 2008; Casadío et al. 2010). As sedimentological data suggest that *Z. marambioensis* sp. nov. and *Z. whangareirensis* lived in shallow-water environments, it seems possible that they were able to tolerate a broader temperature range than other Recent species of the genus, which inhabit cold, deep marine environments.

Regarding changes in depth of habitat, we agree that, considering the current knowledge on the group and the fossil material available, the onshore-offshore theory could apply in this case. Migration to deeper habitats could probably have been related to climate changes occurring in Antarctica during the Oligocene–Miocene. Unfortunately, Oligocene marine rocks preserved in Patagonia (i.e., the San Julián Formation) are not widespread and in all cases do not record deep environments. This kind of environment is not recorded in other post-Eocene deposits either in areas of the southern Atlantic Ocean or areas surrounding Seymour Island, thus limiting our chances of recovering material of *Zoroaster* that could prove such a migration of species of this genus into deeper waters or, conversely, its migration onto shallow water in Antarctica during the Eocene.

## Acknowledgements

Authors acknowledge Carolina Acosta Hospitaleche and Javier Gelfo (both Universidad Nacional de La Plata, Argentina) for helping with the specimens collection in the field; Sergio Marensi (Universidad de Buenos Aires, Argentina) and Carlos Zavala (Universidad Nacional del Sur, Bahía Blanca, Argentina) for the comments on the stratigraphy and sedimentology; and Carolina Martín Cao-Romero (Universidad Nacional Autónoma de México, Ciudad de México, México) for the relevant comments about important characters to differentiate species of the genus. We also thank the very useful comments and suggestions made by the reviewers, Christopher Mah (National Museum of Natural History, Washington, USA), Daniel Blake (University of Illinois, Springfield, USA), and an anonymous. This publication was supported by CONICET and Instituto Antártico Argentino. Funding to this project was provided by Agencia Nacional de Promoción de la Investigación, el Desarrollo Tecnológico y la Innovación (PICT 2018-917).

## References

- Alcock, A. 1893. Natural History notes from the HM Indian Marine Survey Steamer Investigator. An account of the collection of deep-sea Asteroidea. *Annals of the Magazine of Natural History* 11: 73–121.
- Amenábar C.R., Montes M., Nozal F., and Santillana S. 2020. Dinoflagellate cysts of the La Meseta Formation (middle to late Eocene), Antarctic Peninsula: implications for biostratigraphy, palaeoceanography and palaeoenvironment. *Geological Magazine* 157: 351–366.
- Aronson, R.B. and Blake, D.B. 2001. Global climate change and the origin of modern benthic communities in Antarctica. *American Zoologist* 41: 27–39.
- Aronson, R.B., Blake, D.B., and Oji, T. 1997. Retrograde community structure in the late Eocene of Antarctica. *Geology* 25: 903–906.
- Aronson, R.B., Moody, R.M., Ivany, L.C., Blake, D.B., Werner, J.E., and Glass, A. 2009. Climate change and trophic response of the Antarctic bottom fauna. *PLoS ONE* 4: e4385.
- Ausich, W.I., Jangoux, M., and Lawrence, J.M. 2001. Echinoderm taphonomy. In: M. Jangoux and J.M. Lawrence (eds.), *Echinoderm Studies* 6, 171–227. CRC Press, Taylor & Francis Group, Boca Raton.
- Baumiller, T.K. and Gaździcki, A. 1996. New crinoids from the Eocene La Meseta formation of Seymour island, Antarctic peninsula. *Palaeontologia Polonica* 55: 101–116.
- Bijl, P.K., Bendle, J.A., Bohaty, S.M., Pross, J., Schouten, S., Tauxe, L., Stickley, C.E., McKay, R.M., Röhl, U., Olney, M., Sluijs, A., Escutia, C., Brinkhuis, H., and Expedition 318 Scientists 2013. Eocene cooling linked to early flow across the Tasmanian Gateway. *Proceedings of the National Academy of Sciences* 110: 9645–9650.
- Bitner, M.A. 1996. Brachiopods from the Eocene La Meseta Formation of Seymour Island, Antarctic Peninsula. *Palaeontologia Polonica* 55: 65–100.
- Blainville, H.M. de, 1830. *Zoophytes. Dictionnaire des Sciences Naturelles*. 60 pp. F.G. Levrault, Strasbourg.
- Blake, D.B. 1987. A classification and phylogeny of post-Palaeozoic sea stars (Asteroidea: Echinodermata). *Journal of Natural History* 21: 481–528.
- Blake, D.B. 1990. Adaptive zones of the class Asteroidea (Echinodermata). *Bulletin of Marine Science* 46: 701–718.
- Blake, D.B. and Aronson, R.B. 1998. Eocene stelleroids (Echinodermata) at Seymour Island, Antarctic Peninsula. *Journal of Paleontology* 72: 339–353.
- Blake, D.B. and Hotchkiss, F.H. 2004. Recognition of the asteroid (Echinodermata) crown group: implications of the ventral skeleton. *Journal of Paleontology* 78: 359–370.
- Blake, D.B. and Zinsmeister, W.J. 1979. Two early Cenozoic sea stars (class Asteroidea) from Seymour Island, Antarctic Peninsula. *Journal of Paleontology* 53: 1145–1154.
- Blake, D.B. and Zinsmeister, W.J. 1988. Eocene asteroids (Echinodermata) from Seymour Island, Antarctic Peninsula. *Memoirs of the Geological Society of America* 169: 489–498.
- Brett, C.E. 1978. Taphonomy: Sedimentological implications of fossil preservation. In: Middleton G.V., Church M.J., Coniglio M., Hardie L.A., and Longstaffe F.J. (eds.) *Encyclopedia of Sediments and Sedimentary Rocks. Encyclopedia of Earth Sciences Series*, 723–739. Springer, Dordrecht.
- Brett, C.E., Moffat, H.A., and Taylor W.L. 1997. Echinoderm taphonomy, taphofacies and lagerstätten. *Palaeontological Society Papers* 3: 147–190.
- Brusca, R.C. and Brusca, G.J. 2003. *Invertebrates. 2nd Edition*. xix + 936 pp. Sinauer Associates, Sunderland.
- Casadio, S., Nelson, C., Taylor, P., Griffin, M., and Gordon, D. 2010. West Antarctic Rift System: A possible New Zealand-Patagonia Oligocene paleobiogeographic link. *Ameghiniana* 47: 129–132.
- Clark, H.L. 1913. Echinoderms from Lower California, with descriptions of new species. *Bulletin of the American Museum of Natural History* 32: 185–236.
- Clark, H.L. 1916. Report on the sea-lilies, starfishes, brittle-stars and sea-urchins obtained by the F.I.S. “Endeavour” on the coasts of Queensland, New South Wales, Tasmania, Victoria, South Australia, and Western Australia. *Biological Results of the Fishing Experiments Carried on by the F.I.S. Endeavour 1909–1914* 4: 1–123.
- Clark, H.L. 1920. Reports on the scientific results of the expedition to the Eastern Tropical Pacific, in charge of Alexander Agassiz, by the U.S. Fish Commission Steamer “Albatross”, from October, 1904, to March, 1905, Lieut. Commander L.M. Garrett, U.S.N., commanding. *Asteroidea. Memoirs of the Museum of Comparative Zoology at Harvard College* 39: 75–113.
- Clark, A.M. and Downey, M.E. 1992. *Starfishes of the Atlantic*. 792 pp. Chapman & Hall, London.
- Clarke, A. and Johnston, N.M. 2003. Antarctic marine benthic diversity. *Oceanography and Marine Biology* 41: 47–114.
- Douglas, P.M.J., Affek, H.P., Ivany, L.C., Houben, A.J.P., Sijp, W.P., Sluijs, A., Schouten, S., and Pagani, M. 2014. Pronounced zonal heterogeneity in Eocene southern high-latitude sea surface temperatures. *Proceedings of the National Academy of Sciences, USA* 111: 1–6.
- Downey, M.E. 1970. Zoroallida, new order, and *Doraster constellatus*, new genus and species, with notes on the Zoroasteridae (Echinodermata: Asteroidea). *Smithsonian Contributions to Zoology* 64: 1–18.
- Dutton, A.L., Lohmann, K.C., and Zinsmeister, W.J. 2002. Stable isotope and minor element proxies for Eocene climate of Seymour Island, Antarctica. *Paleoceanography* 17 [published online, <https://doi.org/10.1029/2000PA000593>].
- Eagle, M.K. 2006. A new asteroid (Forcipulatida: Zoroasteridae) from the Eocene of Whangarei, Northland, New Zealand. *Records of the Auckland Museum* 43: 81–96.
- Esteban-Vázquez, B.L. 2018. *Biodiversidad de estrellas de mar (Echinodermata: Asteroidea) del estado de Veracruz, México*. 377 pp. B.Sc. Thesis, Universidad Nacional Autónoma de México (UNAM), México DF.
- Fau, M. and Villier, L. 2018. Post-metamorphic ontogeny of *Zoroaster fulgens* Thomson, 1873 (Asteroidea, Forcipulatacea). *Journal of Anatomy* 233: 644–665.
- Fedorov, A., Beichel, R., Kalpathy-Cramer, J., Finet, J., Fillion-Robin, J.-C., Pujol, S., Bauer, C., Jennings, D., Fennessy, F.M., Sonka, M., Buatti, J., Aylward, S.R., Miller, J.V., Pieper, S., and Kikinis, R. 2012. 3D Slicer as an Image Computing Platform for the Quantitative Imaging Network. *Magnetic Resonance Imaging* 30: 1323–1341.
- Feldmann, R.M. and Woodburne, M.O. (eds.) 1988. Geology and Paleontology of Seymour Island, Antarctic Peninsula. *Geological Society of America Memoirs* 169: 1–566.
- Ferguson, J.C. 1992. The function of the madreporite in body fluid volume maintenance by an intertidal starfish, *Pisaster ochraceus*. *Biological Bulletin* 183: 482–489.
- Fisher, W.K. 1905. New starfishes from deep water off California and Alaska. *Bulletin of the Bureau of Fisheries* 29 (for 1904): 291–320.
- Fisher, W.K. 1906. The starfishes of the Hawaiian islands. *Bulletin of the United States Fish Commission* 23: 987–1130.
- Fisher, W.K. 1916. New east Indian starfishes. *Proceedings of the Biological Society of Washington* 29: 27–36.
- Fisher, W.K. 1919. North Pacific Zoroasteridae. *Annals and Magazine of Natural History* 3 (9): 387–353.
- Fisher, W.K. 1928. Asteroidea of the North Pacific and adjacent waters, Part 2: Forcipulata (Part). *Bulletin of the United States National Museum* 76: 1–245.
- Gale, A. 2011. The phylogeny of Post-Paleozoic Asteroidea (Neoasteroidea: Echinodermata). *Special Papers in Paleontology* 85: 1–112.
- Gaździcki, A., Gruszczynski, M., Hoffman, A., Małkowski, K., Marenski, S., Hałas, S., and Tatur, A. 1992. Stable carbon and oxygen isotope record in the Paleogene La Meseta Formation, Seymour Island, Antarctica. *Antarctic Science* 4: 461–468.
- Goin, F.J., Case, J.A., Woodburne, M.O., Vizcaíno, S.F., and Reguero, M.A. 1999. New discoveries of “opossum-like” marsupials from Antarctica (Seymour Island, Medial Eocene). *Journal of Mammalian Evolution* 6: 335–365.
- Goloboff, P.A. and Catalano, S.A. 2016. TNT version 1.5, including a full



- implementation of phylogenetic morphometrics. *Cladistics* 32: 221–238.
- Gozdzak, P., Salamon, M.A., and Baumiller, T.K. 2012. Predator-induced macroevolutionary trends in Mesozoic crinoids. *Proceedings of the National Academy of Sciences of the United States of America* 109: 7004–7007.
- Hara, U. 2001. Bryozoa from the Eocene of Seymour Island, Antarctic Peninsula. *Palaeontologia Polonica* 60: 33–156.
- Hayashi, R. 1943. Contributions to the classification of the sea-stars of Japan. Forcipulata, with the note on the relationships between the skeletal structure and respiratory organs of the sea-stars. *Journal of the Faculty of Science Hokkaido Imperial University, Series VI, Zoology* 8: 133–281.
- Hayashi, R. 1961. Asteroidea of the Second Japanese Antarctic Research Expedition (1957–1958). *Special Publications from the Seto Marine Biological Laboratory* 1: 1–8.
- Hess, H. 1974. Neue Funde des Seesterns *Terminaster cancriformis* (Quenstedt) aus Callovien und Oxford von England, Frankreich und der Schweiz. *Eclogae Geologicae Helveticae* 67: 647–659.
- Howell, K.L., Rogers, A.D., Tyler, P.A., and Billett, D.S. 2004. Reproductive isolation among morphotypes of the Atlantic seastar species *Zoroaster fulgens* (Asteroidea: Echinodermata). *Marine Biology* 144: 977–984.
- Ivany, L.C., Lohmann, K.C., Hasiuk, F., Blake, D.B., Glass, A., Aronson, R.B., and Moody, R.M. 2008. Eocene climate record of a high southern latitude continental shelf: Seymour Island, Antarctica. *Geological Society of America Bulletin* 120: 659–678.
- Kato, M. and Oji, T. 2013. A new species of *Doraster* (Echinodermata: Asteroidea) from the lower Miocene of central Japan: implications for its enigmatic paleobiogeography. *Paleontological Research* 17: 330–334.
- Kidwell, S.M. 1991. Stratigraphy of shell concentrations. In: P.A. Allison and D.E. Briggs (eds.), *Taphonomy: Releasing the Data Locked in the Fossil Record*, 211–290. Plenum Press, New York.
- Limaye, A. 2012. Drishti: volume exploration and presentation tool. In: S.R. Stock (ed.), *Developments in X-Ray Tomography VIII, Proceedings of the SPIE Optical Engineering + Applications*, 85060X. International Society for Optics and Photonics, San Diego.
- Ludwig, H. 1905. Asteroidea. *Memoirs of the Museum of Comparative Zoology at Harvard* 32: 1–292.
- Maddison, W.P. and Maddison, D.R. 2019. *Mesquite: a Modular System for Evolutionary Analysis*. version 3.61; available at <http://www.mesquiteproject.org/>
- Mah, C.L. 2000. Preliminary phylogeny of the forcipulatacean Asteroidea. *American Zoologist* 40: 375–381.
- Mah, C.L. 2007. Phylogeny of the Zoroasteridae (Zorocallina; Forcipulata): evolutionary events in deep-sea Asteroidea displaying Palaeozoic features. *Zoological Journal of the Linnean Society* 150: 177–210.
- Mah, C.L. and Blake, D.B. 2012. Global diversity and phylogeny of the Asteroidea (Echinodermata). *PLoS ONE* 7: e35644.
- Mah, C.L. and Foltz, D. 2011. Molecular phylogeny of the Forcipulatacea (Asteroidea: Echinodermata): systematics and biogeography. *Zoological Journal of the Linnean Society* 162: 646–660.
- Marenssi, S.A., Santillana, S.N., and Rinaldi, C.A. 1998a. Paleoambientes sedimentarios de la Aloformación La Meseta (Eoceno), isla Marambio (Seymour), Antártida. *Contribuciones del Instituto Antártico Argentino* 464: 1–51.
- Marenssi S.A., Santillana, S.N., and Rinaldi, C.A. 1998b. Stratigraphy of the La Meseta Formation (Eocene), Marambio (Seymour) Island, Antarctica. *Asociación Paleontológica Argentina, Publicación Especial* 5: 137–146.
- McKnight, D.G. 2006. The marine fauna of New Zealand, Echinodermata: Asteroidea (Sea-stars). Orders Velatida, Spinulosida, Forcipulata, Brisingida with addenda to Paxillosida, Valvatida. *NIWA Biodiversity Memoir* 120: 1–187.
- Meyer, D.L. and Oji, T. 1993. Eocene crinoids from Seymour Island, Antarctic Peninsula: paleobiogeographic and paleoecologic implications. *Journal of Paleontology* 67: 250–257.
- Meyer, D.L. and Macurda, D.B., Jr. 1977. Adaptive radiation of the comatulid crinoids. *Paleobiology* 3: 74–82. {not cited in the text}
- Montes, M., Nozal, F., Olivero, E., Gallastegui, G., Santillana, S., Maestro, A., López-Martínez, J., González, L., and Martín-Serrano, A. 2019. Geología y Geomorfología de isla Marambio (Seymour). In: M. Montes, F. Nozal, and S. Santillana (eds.), *Serie Cartográfica Geocientífica Antártica; 1:20.000. 1ª edición*. 300 pp. Instituto Geológico y Minero de España, Madrid and Instituto Antártico Argentino, Buenos Aires.
- Montes, M., Nozal, F., Santillana, S., Marenssi, S., and Olivero, E. 2013. *Mapa Geológico de la Isla Marambio (Seymour); escala 1:20.000. Serie Cartográfica Geocientífica Antártica*. Instituto Geológico y Minero de España, Madrid and Instituto Antártico, Buenos Aires.
- Mooi, R. and David, B. 2000. What a new model of skeletal homologies tells us about asteroid evolution? *American Zoologist* 40: 326–339.
- Perrier, E. 1884. Mémoire sur les étoiles de mer recueillies dans la mer des Antilles et le golfe du Mexique durant les expéditions de dragage faites sous la direction de M. Alexandre Agassiz. *Archives. Muséum national d'histoire naturelle, France, sér. 6* 2: 127–276.
- Porębski, S.J. 2000. Shelf-valley compound fill produced by fault subsidence and eustatic sea-level changes, Eocene La Meseta Formation, Seymour Island, Antarctica. *Geology* 28: 147–150.
- Sadler, P.M. 1988. Geometry and stratification of uppermost Cretaceous and Paleogene units on Seymour Island, northern Antarctic Peninsula. In: R.M. Feldman and M.O. Woodburne (eds.), *Geology and Paleontology of Seymour Island, Antarctic Peninsula. Memoirs of the Geological Society of America* 169: 303–320.
- Sladen, W.P. 1889. Report on the Asteroidea. Report on the Scientific Results of the Voyage of H.M.S. Challenger during the years 1873–1876. *Zoology* 30: 1–893.
- Spencer, W.K. and Wright, C.W. 1966. *Asterozoans*. In: R.C. Moore (ed.), *Treatise on Invertebrate Paleontology, Part U, Echinodermata 3 (1)*, 4–107. The Geological Society of America, Inc. and The University of Kansas Press, Lawrence.
- Stilwell, J.D. and Zinsmeister, W.J. 1992. Molluscan systematics and biostratigraphy: lower Tertiary La Meseta Formation, Seymour Island, Antarctic Peninsula. *American Geophysical Union, Antarctic Research Series* 55: 1–192.
- Sumida, P.Y., Tyler, P.A., and Billett, D.S. 2001. Early juvenile development of deep-sea asteroids of the NE Atlantic Ocean, with notes on juvenile bathymetric distributions. *Acta Zoologica* 82: 11–40.
- Swofford, D.L. 2003. *PAUP\*. Phylogenetic Analysis using parsimony (\*and Other Methods)*. Version 4. Sinauer Associates, Sunderland.
- Taylor, P.D., Casadio, S., and Gordon, D.P. 2008. A rare form of frontal shield development in the new cheilostome bryozoan genus *Uharella* from the Eocene of Antarctica. *Paläontologische Zeitschrift* 82: 262–268.
- Villier, L., Charbonnier, S., and Riou, B. 2009. Sea Stars from Middle Jurassic Lagerstätte of La Voulte-sur-Rhône (Ardèche, France). *Journal of Paleontology* 83: 389–398.
- Whittle, R.J., Hunter, A.W., Cantrill, D.J., and McNamara, K.J. 2018. Globally discordant Isocrinida (Crinoidea) migration confirms asynchronous Marine Mesozoic Revolution. *Communications Biology* 1: article 46. [published online, <https://doi.org/10.1038/s42003-018-0048-0>].
- Zavala, C., Arcuri, M., and Blanco Valiente, L. 2012. The importance of plant remains as diagnostic criteria for the recognition of ancient hyperpycnites. *Revue de Paléobiologie* 11: 457–469.
- Zavala, C. and Pan, S.X. 2018. Hyperpycnal flows and hyperpycnites: Origin and distinctive characteristics. *Lithologic Reservoirs* 30: 1–27.
- Zavala, C., Arcuri, M., Di Meglio, M., Gamero Diaz, H., and Contreras, C. 2011. A genetic facies tract for the analysis of sustained hyperpycnal flow deposits. In: R.M. Slatt and C. Zavala (eds.), *Sediment Transfer from Shelf to Deep Water—Revisiting the Delivery System. AAPG Studies in Geology* 61: 31–51.
- Zinsmeister, W.J. 1982. Late Cretaceous–early Tertiary molluscan biogeography of the southern circum-Pacific. *Journal of Paleontology* 56: 84–102.

# Appendix 1

Characters added to the zoroasterid matrix of Mah (2007).

Ch. 71: *Distribution of pedicellariae on abactinal surface*. 0: associated to popular pores, 1: associated to carinals.

Ch. 72: *Size of pedicellariae on abactinal surface*. 0: small, 1: big.

Ch. 73: *Number of actinolateral rows*. 0: three, 1: four, 2: five, 3: six.

Ch. 74: *First actinolateral row differentiated from others*. 0: absent, 1: present.

Ch. 75: *Actinolateral primary spines adpressed*. 0: absent, 1: present.

Ch. 76: *Number of actinolateral pedicellariae*. 0: none, 1: one, 2: more than one.

Ch. 77: *Size of actinolateral pedicellariae*. 0: small, 1: big, 2: pedicellariae absent.

Ch. 78: *Number of pedicellariae on carinate adambulacral innermost spine*. 0: 0-2, 1: 2-5, 2: 5-8, 3: more than 8.

Ch. 79: *Both small and big pedicellariae associated to carinate adambulacrals*. 0: absent, 1: present.